

Article

Synthesis and Self-Assembling Properties of Peracetylated β -1-Triazolyl Alkyl D-Glucosides and D-Galactosides

Pooja Sharma , Anji Chen, Dan Wang and Guijun Wang * 

Department of Chemistry and Biochemistry, Old Dominion University, Norfolk, VA 23529, USA; psharma@odu.edu (P.S.); achen@odu.edu (A.C.); d2wang@odu.edu (D.W.)

* Correspondence: g1wang@odu.edu; Tel.: +1-(757)-683-3781

Abstract: Carbohydrate-based low-molecular-weight gelators (LMWGs) are useful classes of compounds due to their numerous applications. Among sugar-based LMWGs, certain peracetylated sugar beta-triazole derivatives were found to be effective organogelators and showed interesting self-assembling properties. To further understand the structural influence towards molecular assemblies and obtain new functional materials with interesting properties, we designed and synthesized a library of tetraacetyl beta-1-triazolyl alkyl-D-glucosides and D-galactosides, in which a two or three carbon spacer is inserted between the anomeric position and the triazole moiety. A series of 16 glucose derivatives and 14 galactose derivatives were synthesized and analyzed. The self-assembling properties of these new triazole containing glycoconjugates in different solvents were analyzed. Several glucose derivatives were found to be effective LMWGs, with compound **7a** forming gels in a variety of organic solvents as well as in the presence of metal ions in aqueous solutions. The organogels formed by several compounds were characterized using optical microscopy, atomic force microscopy (AFM) and UV-vis spectroscopy, etc. The co-gels formed by compound **7a** with the Fmoc derivative **7i** showed interesting fluorescence enhancement upon gelation. Several gelators were also characterized using powder X-ray diffraction and FT-IR spectroscopy. The potential applications of these sugar-based gelators for drug delivery and dye removal were also studied.

Keywords: glucose; galactose; triazoles; organogelators; metallo gels; self-assembly; supramolecular gels; fluorescence; hydrogelators



Citation: Sharma, P.; Chen, A.; Wang, D.; Wang, G. Synthesis and Self-Assembling Properties of Peracetylated β -1-Triazolyl Alkyl D-Glucosides and D-Galactosides. *Chemistry* **2021**, *3*, 935–958. <https://doi.org/10.3390/chemistry3030068>

Academic Editors: George O'Doherty and Michael D. Ward

Received: 27 June 2021

Accepted: 23 August 2021

Published: 28 August 2021

Publisher's Note: MDPI stays neutral with regard to jurisdictional claims in published maps and institutional affiliations.



Copyright: © 2021 by the authors. Licensee MDPI, Basel, Switzerland. This article is an open access article distributed under the terms and conditions of the Creative Commons Attribution (CC BY) license (<https://creativecommons.org/licenses/by/4.0/>).

1. Introduction

Low-molecular-weight gelators (LMWGs) are interesting small molecules that can self-assemble and form gels in a variety of organic solvents or in water [1–4]. The resulting supramolecular gels are formed through non-covalent forces such as hydrophobic interactions, hydrogen bonding, π - π interactions and CH- π interactions. These gels have demonstrated their potential in a wide range of applications, ranging from biomedical to environment remediation, catalysis, and optical electronic devices [1,2,5]. Low-molecular-weight hydrogelators are especially interesting due to their many applications in biomedical research [6]. Due to the importance of these classes of materials, the rational design and discovery of LMWGs have been an intense field of study. Stimuli-responsive gelators have been explored for different applications in supramolecular chemistry and for organic reactions, the formation of metallo gels further expands the capacity of small organic molecules to have additional properties. For instance, metallo gels formed by LMWGs in the presence of metal ions have found very versatile applications in catalysis and formation of stable nano structures [7–9]. From the assembly of chromophores, aggregation induced emission of gels and their applications for sensing and pollutant removal have also been reported [10]. Aromatic functional groups have been used extensively in the design of hydrogelators, for example the N-fluorenylmethoxycarbonyl (Fmoc) moiety has been used for the design of enzyme triggered hydrogelators [11–14]. Fmoc-modified small molecules

including glucosamine and peptides can self-assemble and form nanofibers driven by π - π stacking of the highly conjugated fluorenyl group. Recently several Fmoc modified small molecule gelators have demonstrated biological properties and utilized for drug delivery applications [15–17]. The fluorescence properties were studied based on different concentrations to help elucidate the self-assembling mechanisms in these systems as well. Therefore, compounds containing the fluorophore may be useful as a fluorescent probe to monitor the structural changes in a self-assembled system of a gel as compared to the corresponding solution form. Among various categories of materials that have shown tendency to form gels, carbohydrate-based gelators are unique since they are derived from materials that are biocompatible, naturally abundant, and inexpensive. Carbohydrate-based LMWGs have gained extensive interests due to their interesting applications in the areas of biomedical sciences, environmental remediation [18–22].

Among the carbohydrate derivatives, 1,2,3-triazole containing compounds are particularly interesting due to the ease of synthesis and the amide-like properties of the triazole heterocycle. Using the copper (I) catalyzed azide alkyne cycloaddition reactions (CuAAC), the “click chemistry”, a variety of carbohydrate and triazole derivatives have been synthesized and they have shown a broad array of applications in synthetic chemistry, medicinal chemistry, biochemistry as well as catalysis [23–25]. The 1,2,3-triazole containing scaffolds can form hydrogen bonds and π - π stacking interactions which make them good candidates for the preparation of self-assembling systems and soft-materials [26]. Furthermore the triazole moieties are useful bioisosteres for drug discoveries, making them an important scaffold for a variety of applications [27]. Recently, several monosaccharide and disaccharide-based triazole derivatives synthesized through click chemistry have been shown to be effective LMWGs [28,29]. We have also found that certain peracetylated D-glucose and D-glucosamine derivatives were effective LMWGs [30,31]. In the rational design of effective supramolecular gelators, several glycoclusters covalently linking triazole containing glycosides were also obtained and showed useful properties for sustained release of vitamins [32] and catalysis [33]. Sugar-based triazole derived organogelators have shown many other applications such as oil spill cleanup and dye removal [34,35].

As shown in Figure 1, a few peracetylated β -triazolyl derivatives of glucose **I** formed organogels in solvents such as toluene and alcohols as well as in the aqueous mixtures of ethanol and dimethyl sulfoxide [30]. These compounds contain the triazole functional group at the anomeric position with different substituents on the triazole ring. The gelation properties showed dependence on the R group functionality such as hydrocarbon chain length, presence of aromatic group or hydroxyl substituent. In addition, peracetylated maltosyl triazole derivatives were found to be effective LMWGs, but the deacetylated maltosyl triazole derivatives were soluble in most polar solvents and aqueous mixtures. Therefore, the presence of the acetyl group was deemed crucial to the gelation properties [28]. In order to discover the structural requirements for effective molecular self-assemblies for acetylated glycosides and understand factors that can be useful in the rational design of organogelators, several derivatives with the general structures **Glu2**, **3** and **Gal2**, **3** were designed and synthesized. These compounds contain a two or three methylene group spacer between the anomeric position and the triazole functional group. The R groups and chain lengths between the sugar and triazole ring can potentially impact gelation properties by moving the triazole ring further away from the carbohydrate skeleton which may afford effective molecular assemblies. From the study, the effect of inserting carbon spacers between peracetylated glycosyl ring and triazole moiety on gelation tendencies of these glycoconjugates as compared to previous studies where triazoles were linked directly to the sugar motif can be obtained and this can allow us to obtain new classes of sugar-based gelators. Besides the glucose derivatives, several D-galactose derivatives were also synthesized, and their gelation properties were analyzed. The structural difference in the stereochemistry between D-glucose and D-galactose is expected to alter their effectiveness as low-molecular-weight gelators.

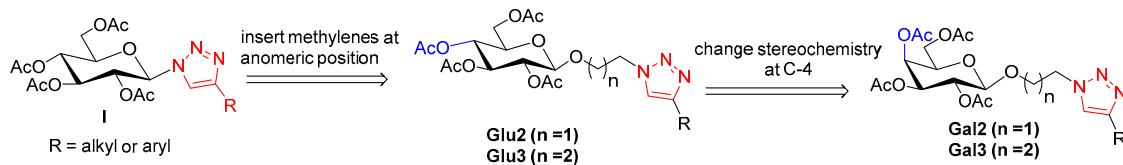
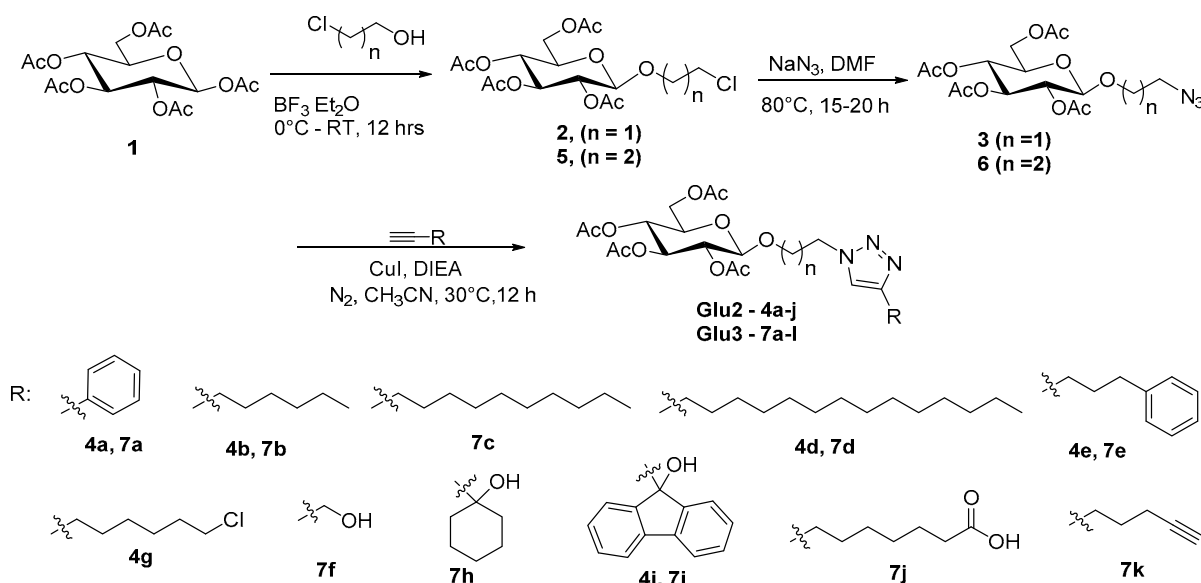


Figure 1. Structures of the glycosyl-triazole conjugates designed from the triazole derivatives with two (**Glu2** and **Gal2**) and three (**Glu3** and **Gal3**) carbon spacers.

2. Results and Discussion

In order to further understand the structural influence on molecular self-assembling and gelation properties, in this study we inserted 2–3 methylene groups between the anomeric center and the triazoles. As shown in Schemes 1 and 2, four series of sugar triazole derivatives containing either two or three carbon spacers were synthesized and characterized. Glycosylation reactions of the pentaacetates of β -D-glucose and β -D-galactose with either chloroethanol or chloropropanol afforded the chloro derivatives **2**, **5** and **9**, **12**. The chloro groups were then displaced with azide to afford intermediates **3**, **6** and **10**, **13**. Using the click reactions, the azides were reacted with various terminal alkynes. The selected alkynes contain different functional groups in the molecules, these ranged from alkyl chain with varying lengths, aromatic, and aliphatic groups with polar functional groups such as hydroxy, carboxyl, chloro at the terminal position. Derivatives containing Fmoc functional groups were also prepared due to the interesting properties of the Fmoc moiety for self-assembling systems.

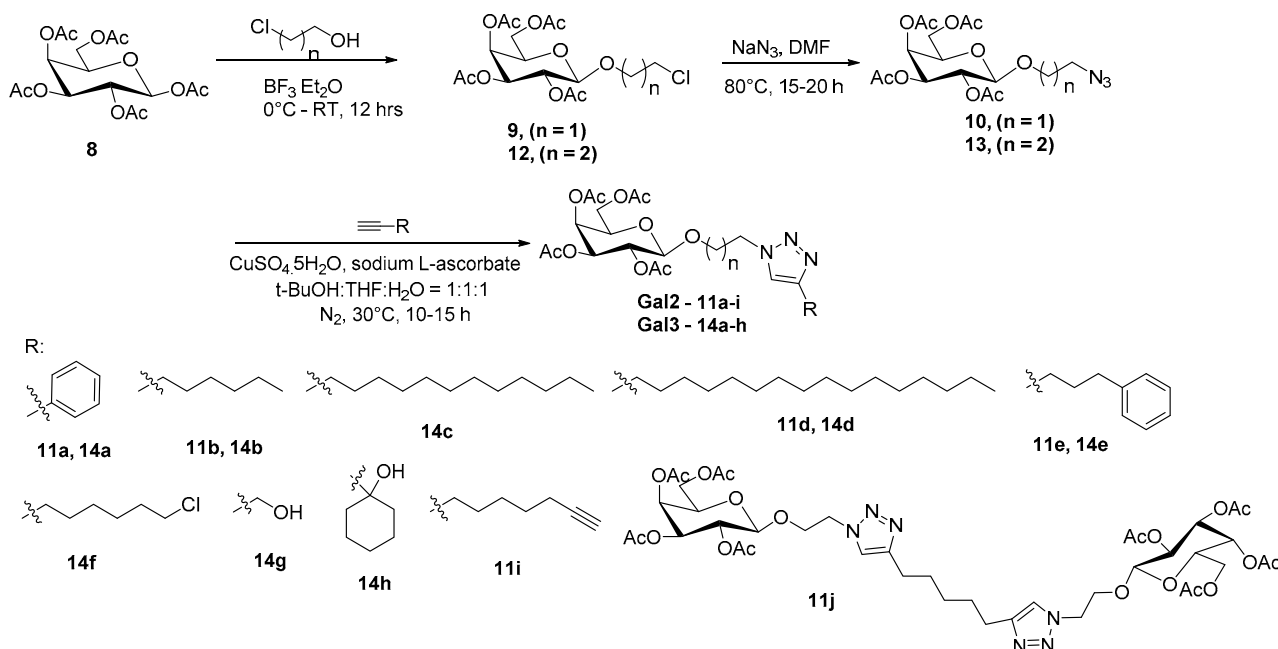


Scheme 1. Synthesis of peracetylated β -triazolyl glucosides **Glu2** (**4a–i**) and **Glu3** (**7a–k**) series.

2.1. Gelation Properties

After the synthesis and purification of the triazole derivatives, their gelation properties in several solvents were tested and the results are shown in Table 1, Tables S1 and S2 (Supplementary Materials). Figure 2 shows some representative photos of the gels formed by these compounds, they typically formed opaque gels. A careful analysis of the gelation results reveals that glucose triazole derivatives having either aromatic ring or long chain aliphatic group were effective gelators and formed several gels in aqueous mixtures of dimethyl sulfoxide and ethanol. For instance, glucose derivatives with 3-carbon spacer and aromatic triazole, compound **7a**, formed a gel at 2.2 mg/mL in DMSO:H₂O (1:2), it also formed precipitates that contained gel-like particles in water. Compound **7c** with a

linear decyl chain formed a gel at 3.3 mg/mL in DMSO:H₂O (1:1), and compound **7d** with a linear tetradecyl substituent, formed a gel at 2.8 mg/mL in EtOH:H₂O (1:1). However, the corresponding analogs with two carbon spacer were not as efficient, they formed gels at relatively higher concentrations. For example, the phenyl triazole **4a** formed a gel at 10.0 mg/mL in DMSO:H₂O (1:2) and EtOH:H₂O (1:2). Gels were also formed in alcohols such as iso-propanol by compounds **4b** and **7a** at 20.0 mg/mL and ethylene glycol by compounds **7c** at 4.0 mg/mL and **4d**, **7d** at 10.0 mg/mL. In addition to this, the triazole derivatives with polar functional groups, such as -OH, -COOH, -Cl groups attached to the triazole subunit, were soluble in most of the solvents tested (Table S1). Other analogs in this series including both the two and three carbon spacers were also mostly soluble in the tested solvents at 20.0 mg/mL. This trend is quite different from what was observed before with the peracetylated glycosyl triazoles [30], in which the 1-hydroxyl cyclohexyl derivative was an effective gelator for several solvents, the insertion of a short alkyl spacer between the anomeric center and the triazole apparently increased the structural flexibility therefore leading to better solubility and not gelation. However, the anomeric phenyl triazole derivative (**I**, R = Ph) was not an effective gelator, it formed mostly precipitate in aqueous mixtures of ethanol and DMSO. The insertion of a two-carbon spacer leads to compound **4a**, this resulted in a more effective gelator for several aqueous mixtures at 10.0 mg/mL while the insertion of a three-carbon spacer (compound **7a**) has resulted in an even more effective gelator, forming gels in five of the tested solvents and some at lower concentrations. While comparing the glucoside triazole derivatives with their galactoside analogs, it was found that the glucose derivatives were more effective gelator as compared to their galactose analogs which were found to be mostly soluble or precipitating in most of the solvents systems (Table S2). This difference can be attributed to the difference in stereochemistry at C-4 position of the sugar rings. In general, the derivatives with polar functional groups such as -OH, and -Cl are soluble in most of the tested solvents and the derivatives with hydrophobic chains perform much better.



Scheme 2. Synthesis of peracetylated β -triazolyl galactosides Gal2 (**11a–j**) and Gal3 (**14a–h**) series.

Table 1. Gelation test results of various triazole derivatives.

No.	<i>i</i> -PrOH	EtOH:H ₂ O (1:1)	EtOH:H ₂ O (1:2)	DMSO:H ₂ O (1:1)	DMSO:H ₂ O (1:2)	Glycerol	Ethylene Glycol	H ₂ O
4a	S	S	G 10.0 _O	G 10.0 _O	G 10.0 _T	S	G 20.0 _O	I
4b	G 20.0 _C	S	I	G 20.0 _O	G 20.0 _T	S	S	I
4d	S	G 10.0 _O	S	G 10.0 _O	P	S	G 10.0 _O	P
7a	G 20.0 _O	S	G 6.7 _O	G 4.0 _O	G 2.2 _O	S	S	PG 5.0 _O
7b	S	S	S	G 10.0 _O	P	S	S	I
7c	S	G 10.0 _O	G 20.0 _O	G 3.3 _O	G 4.0 _O	G* 5.0 _O	G 4.0 _O	P
7d	S	G* 2.8 _O	PG 20.0 _T	PG 20.0 _O	PG 20.0 _O	S	G* 10.0 _O	P

All compounds were tested starting from 20 mg/mL. PG, partial gel at room temperature, G, stable gel at room temperature, the numbers are minimum gelation concentrations (MGCs) in mg/mL; P, precipitation; S, soluble; I, insoluble; G*, gels were formed after 10–12 h of standing at room temperature. Gel appearance: C for clear or transparent; T, translucent; O, opaque. All compounds were soluble in toluene.

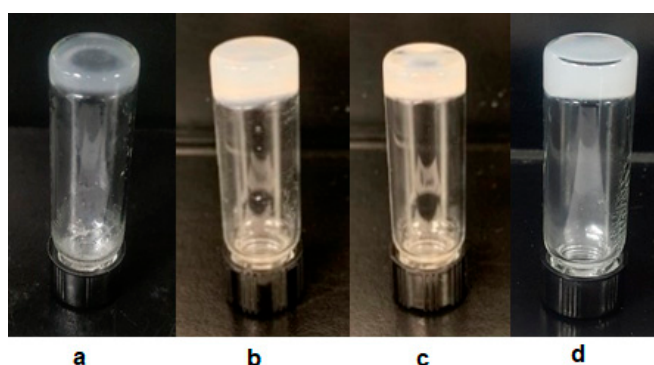


Figure 2. The gels formed by several compounds. (a) A translucent gel formed by compound **4d** in DMSO: H₂O (1:1) at 10.0 mg/mL; (b) an opaque gel formed by compound **7c** in DMSO:H₂O (1:1) at 3.3 mg/mL; (c) an opaque gel formed by compound **7c** in glycerol at 5.0 mg/mL; (d) an opaque gel formed by compound **7d** in EtOH:H₂O (1:1) at 3.3 mg/mL.

The stability of the gels was analyzed by studying their rheological properties. The rheological properties for the gels formed by compounds **4d** and **7d** are shown in Figure 3. These were carried out using 1% strain based on the amplitude sweep results shown in Figure S1a–c. All of them were found to be stable gels with considerable viscoelastic properties since they showed G' values higher than the corresponding G'' values. The data for G'/G'' for the gels are provided in Tables S6–S8 and the average G'/G'' values are 7.06, 8.12, and 2.62 for **4d** in DMSO:H₂O (1:1), **7d** in ethylene glycol, and **7d** in EtOH:H₂O (1:1), respectively. The gel formed by compound **4d** in DMSO:H₂O (1:1) showed the highest G' values followed by **7d** in EtOH:H₂O (1:1). The EtOH:H₂O gel exhibited the lowest overall G'/G'' values among the three, which indicated that the mechanical strength of the other two gels were much higher. These are higher or comparable to the glucosyl triazole derivatives reported before in general (Table S9), with G'/G'' values of 2–4.

2.1.1. Characterization of Gel Morphology

To gain insight into the superstructures formed by the glycoconjugates, the morphologies of these gels were studied using Optical Microscope (OM) and Atomic Force Microscopy (AFM). Since compounds **7a**, **7c** and **7d** were found to be the most effective gelators among the compounds synthesized, the gels formed by these molecules in various solvents were analyzed. The optical micrographs of the gels formed by several compounds are shown in Figure 4. The compound **7a** formed stable gels in DMSO:H₂O (1:1) at 4.0 mg/mL (Figure 4a), the morphology showed uniform long fibrous systems, the fibers appeared over 200 μm in length and about 0.7 μm in diameters; the fibers also were straight and showed stacking or overlapping with other fibers. Figure 4b shows the morphology of the dried gels formed by compound **7c** in DMSO:H₂O (1:1) at 3.3 mg/mL, they formed

flatter sheet rather than fibers or tubules such as compound **7a** in the same solvent system. The assemblies showed clusters of flat long ribbons which are highly birefringent, they appeared bright colored under crossed polarizers (Figure 4b). The same compound **7c** in DMSO:H₂O (1:2) at 4.0 mg/mL showed similar morphology, with a collection of long flat ribbons and some fibers, the planar sheets seemed to be wider compared to Figure 4b, a typical image is shown in Figure 4c. The gel of compound **7d** in EtOH:H₂O (1:1) at 3.3 mg/mL formed similar long straight fibers or cylindrical tubules as well as some planar ribbons. These are also highly birefringent reflecting the chirality in the structures.

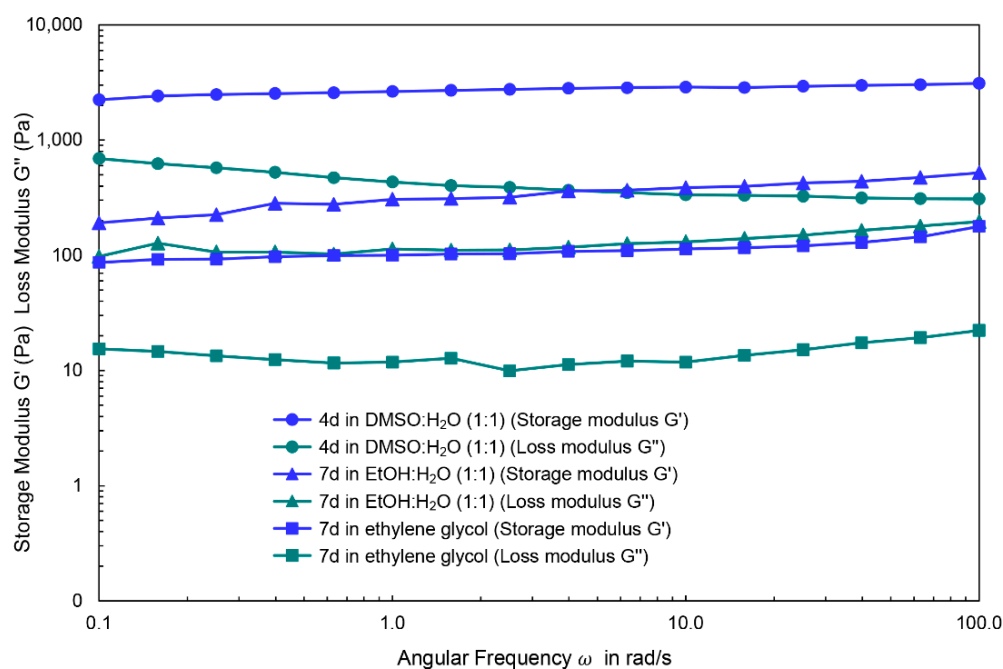


Figure 3. The rheological data for the gels formed by compound **4d** in DMSO:H₂O (1:1) at 10.0 mg/mL, **7d** in EtOH:H₂O (1:1) at 3.3 mg/mL and **7d** in Ethylene glycol at 10.0 mg/mL. The strain was 1% for all samples.

The gels formed by compounds **7c** and **7d** were also analyzed using AFM, the representative images are shown in Figure 5. The gel formed by compound **7c** in DMSO:H₂O (1:1) exhibited densely packed network of long fibers under optical microscope, these are also observed under Atomic Force Microscope which showed the presence of flat sheets (Figure 5a,b). For the gel formed by **7d** in EtOH:H₂O (1:1), it showed similar pattern of planar sheets stacking on top of each other, the long fibers bundle together and form stacked sheet such as morphology (Figure 5c,d). Additional AFM images are shown in Figure S2.

The gel formed by compound **7a** in EtOH:H₂O (1:2) was further examined using FTIR imaging microscopy, a useful tool for analyzing chemical structures of heterogenous materials [36]. The method can allow the direct observation of the gels in presence of solvents. The results are shown in Figure 6, the averaged FTIR spectra of fibers inside the box showed several distinctive signals, 1732 cm⁻¹ for carbonyl group, 1214 cm⁻¹ for C-O stretch and broad signals around 1000 cm⁻¹ correspond to the C=C bending of monosubstituted aromatic group and C-H bending vibrations from 1,3 disubstituted triazole ring. In comparison to the FTIR absorbance of the solid sample of compound **7a** (SI Figure S9B), in which the C=O signal appeared at 1744 cm⁻¹ and C-O stretch at 1225 cm⁻¹, the signal from IR imaging of the fibers showed about 11–14 cm⁻¹ shift.

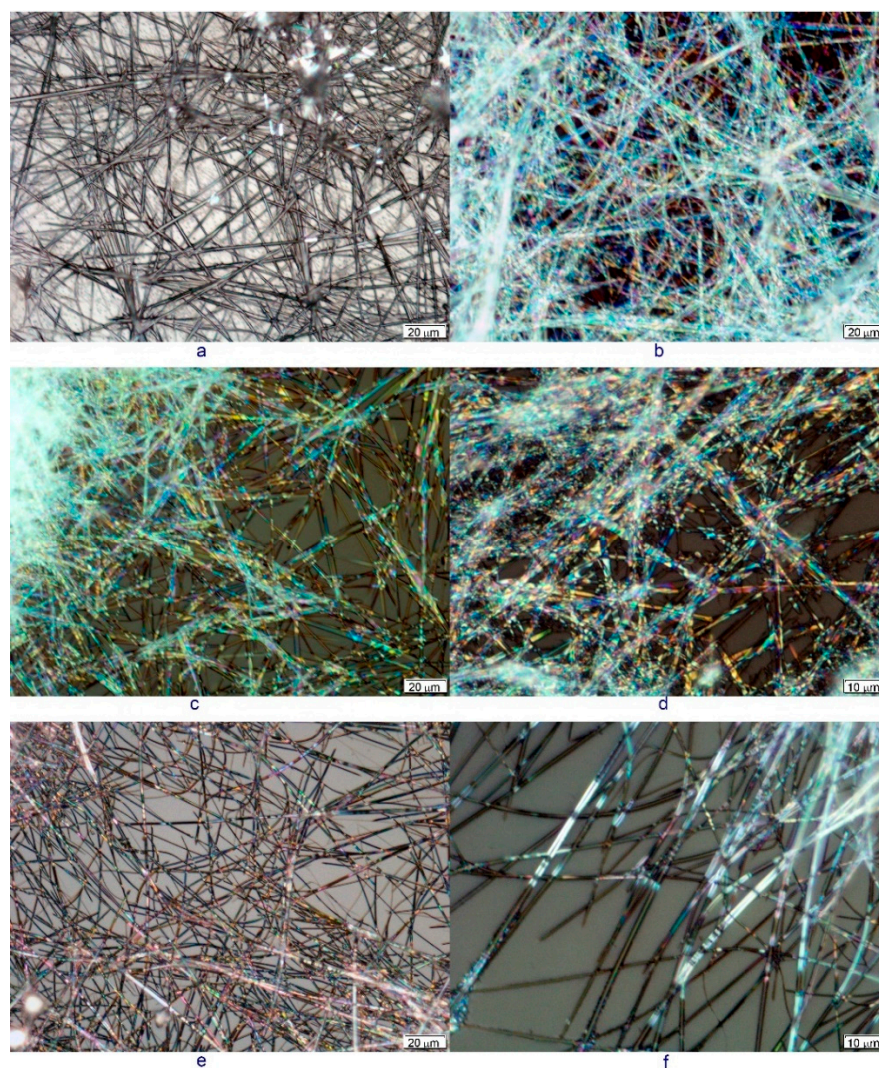


Figure 4. Optical micrographs of several gels formed by different gelators: (a) **7a** in DMSO:H₂O (1:1) at 4.0 mg/mL; (b) **7c** in DMSO:H₂O (1:1) at 3.3 mg/mL; (c) **7c** in DMSO:H₂O (1:2) at 4.0 mg/mL; (d) **7d** in EtOH:H₂O (1:1) at 3.3 mg/mL; (e) **7a** and Ni(OAc)₂·4H₂O (1.5 equiv of **7a**) in DMSO:H₂O (1:5) at 5.0 mg/mL, (f) **7a** and Zn(OAc)₂·2H₂O (1.5 equiv of **7a**) in DMSO:H₂O (1:5) at 4.3 mg/mL.

2.1.2. Co-Gel Formation with Metal Ions

To further study the molecular self-assembling properties, the gelator **7a** was tested in the presence of metal ions. Several metal salts were tested in DMSO and water (*v/v* 1:5), including Hg(OAc)₂, Ni(OAc)₂·4H₂O, Zn(OAc)₂·2H₂O, Pb(OAc)₄, Cu(OAc)₂·H₂O, CuSO₄·5H₂O and CuCl₂. Without these metal salts, compound **7a** formed a stable gel at 6.0 mg/mL (ESI, page S41). In the presence of either 1.0 or 1.5 equiv. of metal salts, gelator **7a** was able to form stable gels with Hg²⁺, Zn²⁺, Ni²⁺ and Pb⁴⁺ salts (Table 2), several photos are shown Figure 7. However, **7a** was soluble and unable to form gels in the presence of any of the three copper salts. The optical micrographs of the metallogels for Ni(OAc)₂, Zn(OAc)₂ are shown in Figure 4f,g, the metallogels showed fibrous network with smaller diameter. The addition of the metal ions seemed to be beneficial for the formation of one-dimensional fibrous network. The formation of stable metallogels could lend them into applications in sensing, catalysis, etc. The metallogels for zinc acetate and nickel acetate were analyzed using FTIR spectroscopy (Figure 8). The vibrational frequency for several functional groups showed small changes after gel formation. The C=O peak shifted from 1744 to 1746 cm⁻¹, and C-O peak changed from 1225 to 1230 cm⁻¹. Other

peaks at 1380 and 979 cm^{-1} corresponding to C-H and C=C bends, respectively, were broader after the formation of the gels.

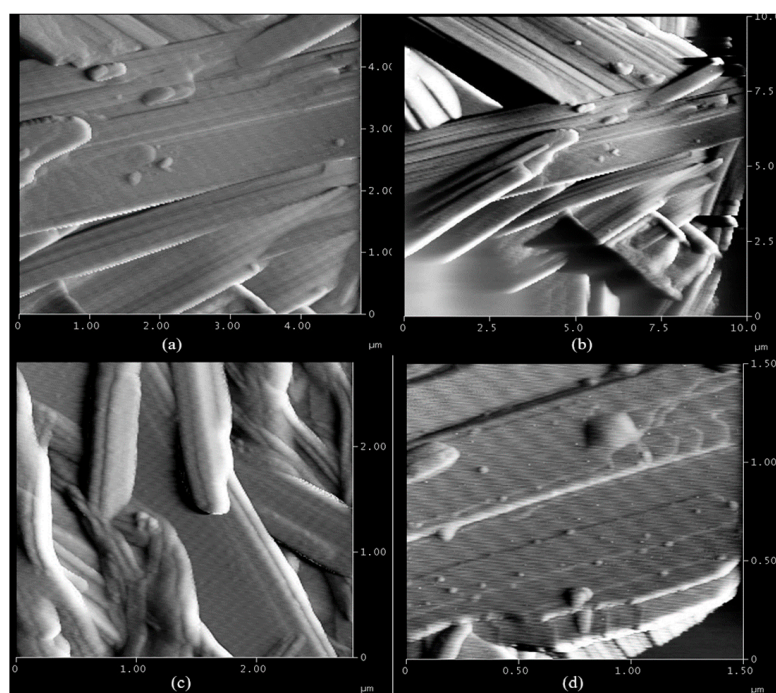


Figure 5. AFM images of the gels formed by compound **7c** and **7d**. (a,b) **7c** in DMSO:H₂O (1:1) at 3.3 mg/mL; (c,d) **7d** in EtOH:H₂O (1:1) at 2.8 mg/mL.

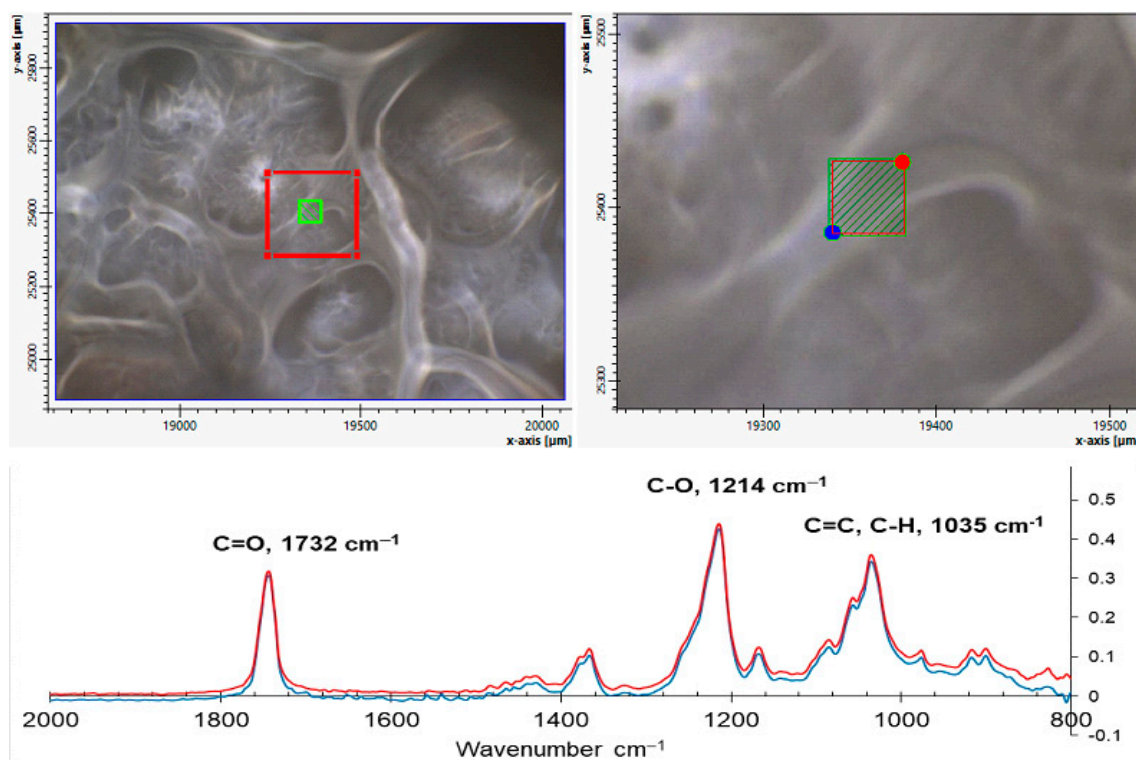
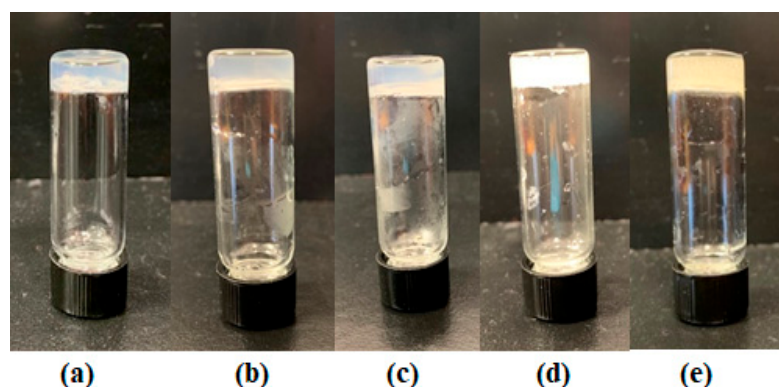
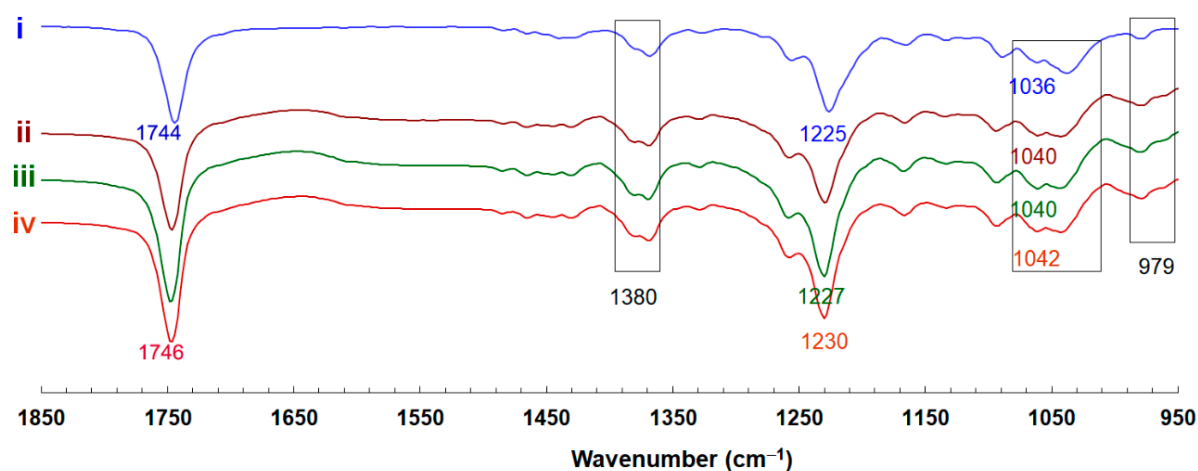


Figure 6. IR imaging spectra of the gel formed by compound **7a** at 10.0 mg/mL in EtOH:H₂O (1:2), the bottom are absorbance IR spectra of the areas marked inside the box.

Table 2. Gelation test results of compound **7a** in the presence of various metal salts.

Metal Acetates	DMSO:H ₂ O (<i>v/v</i>)	1.5 Eq. Metal Acetate Gel mg/mL	1.0 Eq. Metal Acetate Gel mg/mL
Hg(OAc) ₂	1:5	G 6.0	G 6.0
Zn(OAc) ₂ ·2H ₂ O	1:5	G 4.3	G 6.0
Ni(OAc) ₂ ·4H ₂ O	1:5	G 5.0	G 6.0
Pb(OAc) ₄	1:5	G 4.3	G 6.0

**Figure 7.** The gels formed by compound **7a** and its metallogels with different metal ions in DMSO:H₂O (*v/v* 1:5). (a) Compound **7a** at 6.0 mg/mL; (b) **7a** with 1.5 equiv of Ni(OAc)₂·4H₂O at 5.0 mg/mL; (c) **7a** with 1.5 equiv of Zn(OAc)₂·2H₂O at 4.3 mg/mL; (d) **7a** with 1.5 equiv of Hg(OAc)₂ at 6.0 mg/mL; (e) **7a** with 1.5 equiv of Pb(OAc)₄ at 4.3 mg/mL.**Figure 8.** Overlay of the IR spectra of gelator **7a** as solid (i), the gels formed by the compound **7a** in DMSO:H₂O (*v/v* 1:2) at 6.0 mg/mL for ii-iv. (ii) the gel of compound **7a** without any metal salt; (iii) the metallogels of compound **7a** with Ni(OAc)₂·4H₂O (1.5 equiv of **7a**); (iv) the metallogels of compound **7a** with Zn(OAc)₂·2H₂O (1.5 equiv of **7a**).

The stability of the metallogels versus the hydrogels were analyzed using a rheometer and the results are shown in Figure 9. The amplitude sweep results and G' and G'' values are included in ESI Figure S1d-f and Table S10. These three gels displayed viscoelastic properties since all showed higher G' values than the corresponding G'' values. The gel of **7a** in DMSO:H₂O (1:5) had highest G' values, however the G'/G'' values for the metallogels were about two fold higher, the average G'/G'' values for **7a** control, **7a** with nickel acetate, and **7a** with zinc acetate are 1.54, 2.85 and 3.33, respectively. The presence of the metal salts seemed to enhance the mechanical strength of the gels.

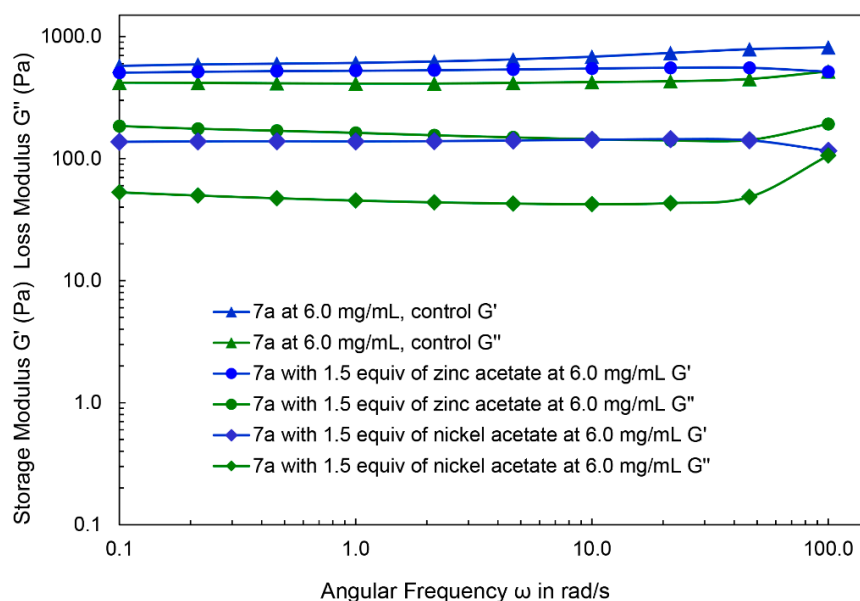


Figure 9. The rheological properties of the gels formed by compound **7a** and its metallogels in DMSO:H₂O (1:5), obtained at 1% strain. The concentrations are 6.0 mg/mL for **7a** in all three.

2.1.3. Naproxen Trapping and Release Study

The effective gelators were analyzed for potential applications for sustained drug delivery. For this application, it is necessary for the gelator to be able to form co-gels with the target drug compounds. The phenylacetylene derivative **7a** was used as the gelator and naproxen was used as the model drug. Naproxen acid contains aromatic functional group and may interact with the gelators through multiple interactions, therefore, resulting in co-gelation with compound **7a**. We found that naproxen formed stable co-gels with compound **7a** in DMSO:H₂O (*v/v* 1:5) at 8.0 mg/mL for **7a** and 0.25 mg/mL for naproxen. The UV-vis absorption spectra of naproxen were utilized to monitor the timed release of the entrapped drug from gel to solution phase. The results are shown in Figure 10, approximately 50% naproxen was released from the gel phase to the aqueous solution after 12 h, and about 95% of the naproxen was released after 50 h. The gel remained intact throughout the study, several photographs of the gels are included in SI Figure S4.

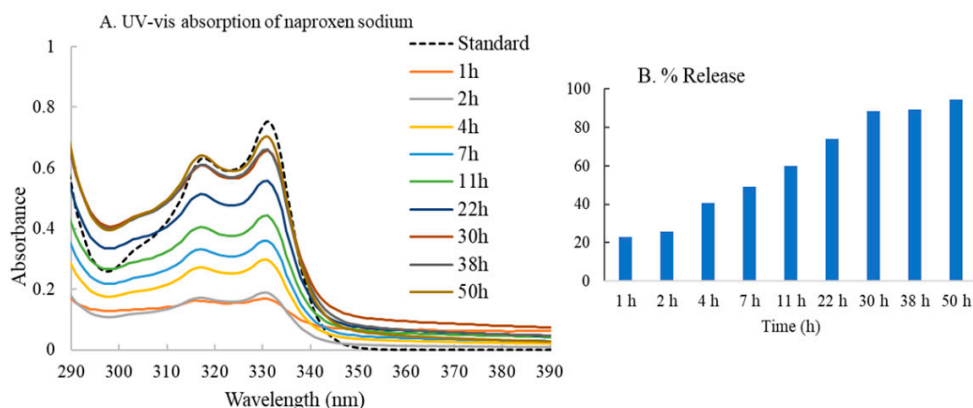


Figure 10. (A) UV-vis absorption spectra of naproxen sodium from the aqueous phase added on top of the gel at different times. (B) The estimated percent release of the drug from the gel. The absorption at 330 nm was used to calculate the amount of drug released. Formula used: % Drug released = $[A_{\text{solution}}/A_{\text{standard}}] * 100$.

2.1.4. Dye Diffusion and Absorption Study

Besides the drug entrapment and its sustained release studies, we also carried out dye absorption studies using toluidine blue dye. As shown in SI Figures S5 and S6, the gel formed by compound **7a** in DMSO:H₂O (*v/v* 1:5) at 8.0 mg/mL was able to absorb the dye slowly, approximately 65% from aqueous phase was removed in 5 days. The gel was further tested for its capacity in dye absorption from a mixture of two dyes: toluidine blue (TB) and methyl orange (MO). The aqueous mixture of the two dyes was added on top of the gel. The UV-vis absorption of the aqueous phase was monitored for a period of 10 days (Figure 11). Additionally, it was estimated that 57% TB and 82% of MO were absorbed by the gels (SI Figures S7 and S8).

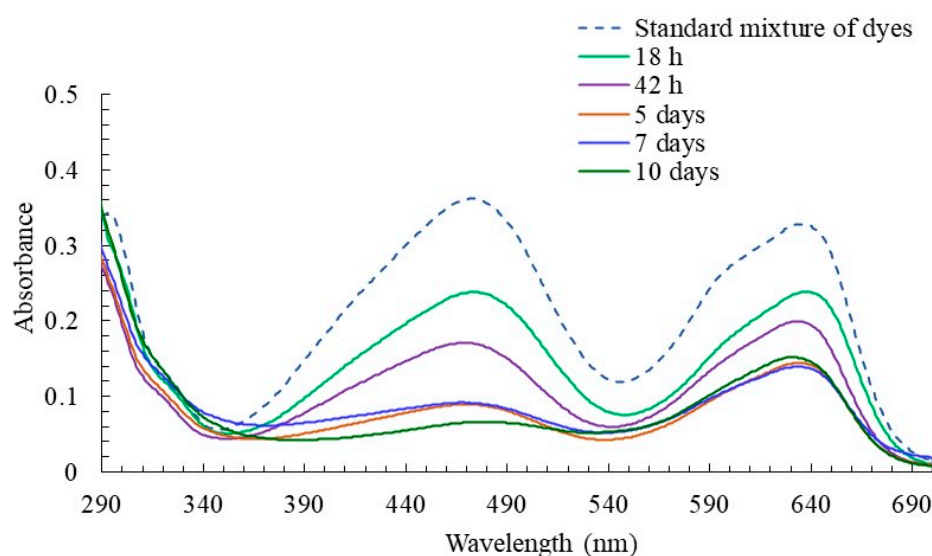


Figure 11. UV spectra of dye solution added on top of the gel compound **7a** at 8.0 mg/mL in DMSO:H₂O (*v/v* 1:5) monitored over time. The standard solution of 0.02 mM toluidine blue and 0.012 mM methyl orange were used. The absorption at 635 nm for Toluidine Blue and 465 nm for Methyl Orange were used to calculate the percentage of dye absorbed. Formula used: % Dye absorbed = $100 - [(A_{\text{solution}})/A_{\text{standard}}] * 100$.

2.1.5. Fluorescent Co-Gels Formed by Compounds **7a** and **7i**

The Fmoc derivative **7i** contains a fluorescent marker, but the compound was not able to form a gel in the tested solvents. However, a co-gel by combining the gelator **7a** with compound **7i** could be obtained. The two-component gel was prepared using compound **7i** (9.1 mol%) and **7a** (91 mol%) in DMSO:H₂O (1:2) as shown in Figure 12a. The fluorescence of the co-gel as observed under UV lamp (365 nm) is shown in Figure 12b. The fluorescence properties of the resulting gel as well as the control gel of **7a** and compound **7i** are shown in Figure 12c. The compound **7i** on its own exhibited a weak emission signal at 448 nm, however, after forming co-gel with **7a**, the intensity increased significantly. This can be attributed to the intermolecular π - π stacking effect of the aromatic groups and intermolecular hydrogen bonding leading to aggregation induced emission enhancement [37] during the formation of the co-gel [38]. In addition to this, the λ_{max} for the co-gel was slightly blue shifted to 444 nm in comparison to the λ_{max} of **7a** at 436 nm and **7i** at 448 nm. Increase in the intensity can be observed in the solution form as well (SI Figure S3) under similar conditions. This indicates that the co-assembly of Fmoc triazole derivative **7i** with the phenyl triazole derivative resulted in stronger fluorescence and the co-gel can be used as potential fluorescent probe.

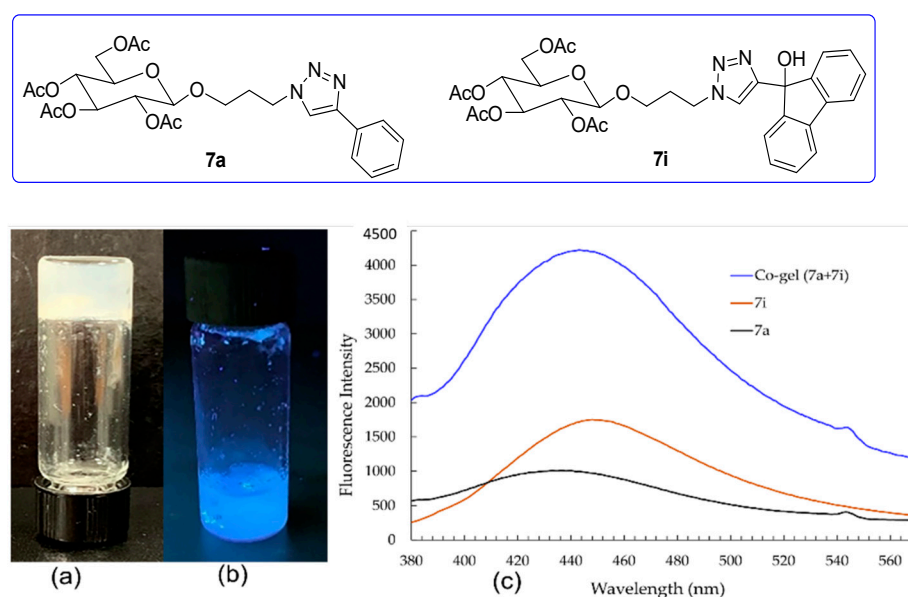


Figure 12. (a) A co-gel of compounds **7a** (10.0 mg/mL) and **7i** (1.2 mg/mL) in DMSO:H₂O (1:2), (b) the same gel under 365 nm UV light. (c) Fluorescence spectra of compound **7i** at 1.2 mg/mL and **7a** at 10.0 mg/mL in DMSO:H₂O (1:2) and the co-gel in (a).

2.1.6. Response to Basic Conditions of Gels Formed by Compound **7c**

The gelators contain acetyl groups which can be hydrolyzed under basic conditions. The gel formed by compound **7c** was treated with basic solution (pH 12). The gel was found to degrade within 4 h partly due to deacetylation reaction, which was confirmed by ¹H NMR analysis of the compound extracted after the gel to solution transition (SI Figures S12–S14). The fully deprotected compounds of **7c** and **14c** were also prepared and tested for gelation, they were not able to form gels in solvents such as ethanol, water and aqueous mixtures of ethanol and DMSO (Table S13). This shows the potential of these molecules as stimuli responsive gels even though the gel to sol transition was irreversible.

2.1.7. Powder XRD Analysis of Compounds **7a** and **7d**

The structures of the gelators **7a** and **7d** were characterized using powder X-ray diffraction, as shown in Figure S10. The two compounds showed distinctive sharp peaks (of 2θ versus the intensity) which indicate the partial crystallinity for both gelators. The PXRD results for the xerogels formed by gelators **7a** and **7d** are shown in Figure 13. The *d* spacing values for both solids and xerogels are included in Tables S11 and S12. The PXRD patterns of the solids and xerogels are significantly different from each other which suggests that gelation induces noticeable changes in the structural arrangement of these molecules. The gelator **7a** showed distinctive peaks in both xerogels and in the solid form, the diffraction patterns indicated the resemblance of the structures in the gel form as compared to the solid, both indicating ordered layered structures. The xerogel of **7a** showed much more ordered packing than **7d**, reflecting certain crystallinity in the assembly. The length of **7a** is estimated to be 19.8 Å (Figure S11), in the solid form a peak at 25.3 Å was observed which was not seen in the xero gel. The significant *d* spacing values in the xero gel are 9.7, 8.9, 8.7, 7.9, 7.6, 5.4, 4.2, 3.8 Å; these are observed due to the ordered assembly resulting from intermolecular π-π interactions of the phenyl ring and triazole. The xerogel of **7d** on the other hand, showed much broader and fewer signals. The most distinctive peak is 35.3 Å, which is close to the length of the molecule (32.2 Å). This indicated that the compounds packed in extended conformation and showed layered structures. The other signals corresponding to the sugar rings are also labeled in Figure 13 and these were observed in the XRD of the xerogel. However, a more comprehensive analysis of the crystal structure would be required to interpretate all peaks.

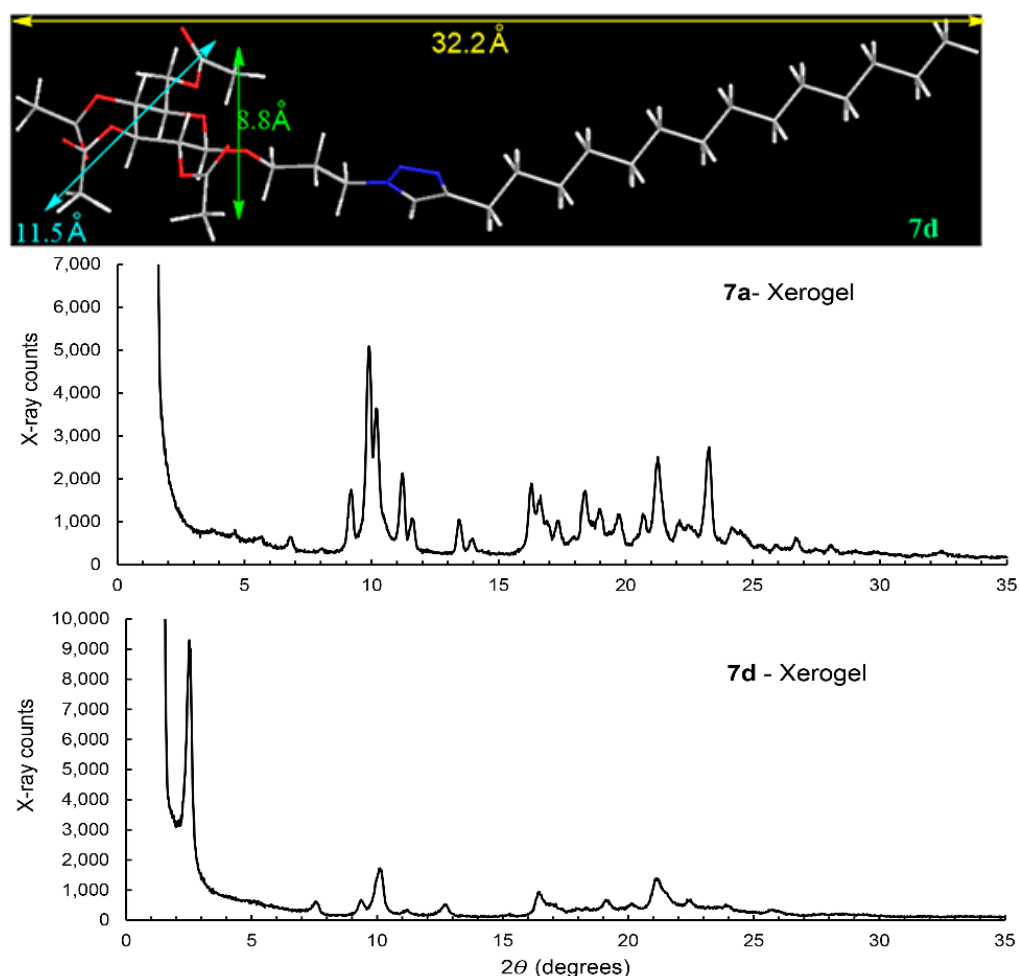


Figure 13. PXRD spectra of xerogels formed by gelators **7a** in EtOH:H₂O (1:2) at 20.0 mg/mL and **7d** EtOH:H₂O (1:1) at 6.0 mg/mL, and the structure of **7d** generated by Chem3D modeling showing the measured distances.

3. Experimental Details

Reagents and solvents were used as they were received from the suppliers. All purification was conducted by flash chromatography using 230–400 mesh silica gel. The solvent systems used for chromatography and for gelation test are all in volume ratios. NMR analysis was conducted using a 400 MHz Bruker NMR spectrometer. The molecular mass was measured using LCMS on an Agilent 6120B Single Quad Mass Spectrometer and LC1260 system or Shimadzu LCMS-2020 with ESI in positive ionization mode. Melting point measurements were carried out using a Stuart automatic melting point apparatus SMP40.

General method for gelation testing: About 2.0 mg of dried compound was placed in a one-dram glass vial and the corresponding solvent was added to obtain a concentration of 20.0 mg/mL. The mixture was then heated until the solids were fully dissolved, sometimes sonication was needed to dissolve the sample, then the solution was allowed to cool to room temperature and let stand for 15 min. After this period, if the sample is a clear solution, this is recorded as soluble, if solid reappeared, this is recorded as precipitate; if the sample formed a gel, then the vial is inverted and if no solvent flowing was observed, this is recorded as a stable gel, otherwise it is recorded as unstable gel. The stable gel was then serially diluted till the minimum gelation concentration, which is the concentration prior to unstable gelation, is obtained.

Metallogel testing method: In a one-dram vial, 3.0 mg of the gelator **7a** (5.6×10^{-3} mmol) was dissolved in 0.5 mL DMSO:H₂O (*v/v* 1:5) mixture. To the mixture, increasing amount of metal salt, 1.0 and 1.5 eq. with respect to the gelator were added. The final mixture was

heated and allowed to cool on bench top without any disturbance. Gelation was tested by inverting the vial.

Optical microscopy studies: A small amount of the gel was placed on a clean glass slide using micro spatula, the gel was air dried but may still contain some solvents and this was observed under an Olympus BX60M optical microscope and the Olympus DP73-1-51 high performance 17MP digital camera with pixel shifting and Peltier cooled. The imaging software for image capturing is CellSens 1.11.

Atomic force microscopy studies: AFM images were acquired using Veeco Dimension 3100 Atomic Force Microscope. The tips used were Tap300-G silicon AFM probes with a resonant frequency of 300 KHz and a force constant of 40 N/m. The samples were prepared by spreading the gel on a glass plate with the help of a micro spatula which was then air dried to obtain corresponding xerogel.

FTIR studies and IR imaging microscopy: FTIR spectroscopy data was collected using Bruker Alpha FTIR spectrometer using OPUS software. Solids were used as such. For gels, a small piece of gel was placed on the plate and background scans were performed with the solvent in which the gel was prepared. IR microscopy was done using Bruker LUMOS-II installed with ATR channel. Detector used for this study was Focal Point Array (FPA)— 32×32 with ZnSe beam splitter. IR images were taken for the gel and its corresponding xerogel.

Rheological analyses: Rheological properties of gels were investigated by HR-2 Discovery Hybrid Rheometer from TA instrument with the TRIOS software or Anton Parr MCR 302 with RheoCompass software. The cone geometry is 25 mm Peltier plate for both and with a gap of 100 μm for HR-2 Rheometer and 1.0 mm for Anton Parr Rheometer. The experimental temperature was 25.0 $^{\circ}\text{C}$, the sample was subjected to amplitude sweep for oscillation strain from 0.125% or 0.1% to 10%. A frequency sweep was then performed for the sample in the range of 0.1 to 100.0 rad/s for angular frequency. The results were expressed as the storage modules (G') and loss modules (G'') as a function of the angular frequency.

PXRD analysis: Bruker D2 Phaser X-ray powder diffractometer installed with Bragg-Brentano optics and Lynx Eye position sensitive detector (PSD) was utilized. The instrument has 1 mm divergence slit, 1 mm anti-scatter air screen and 3 mm detector slit. Silicone low background sample holder was used with 2.5 cm diameter with 0.2 mm depth. The powder was ground on agate mortar with pestle to reduce the crystallite size and the sample holder was not completely covered with powder. For each sample, 2θ ranges from 1.5 $^{\circ}$ or 2 $^{\circ}$ to 35 $^{\circ}$ or 60 $^{\circ}$ with 0.02 $^{\circ}$ step size at 2 scans/step counting time at 15 rpm. PSD opening was set at 0.25 $^{\circ}$ for sample 7a and 0.5 $^{\circ}$ for samples 7d and 7i. Graphs were plotted using Graph Version 12.

Fluorescent co-gels formed by compounds 7a and 7i: Fluorescence emission spectra was obtained using Shimadzu RF-6000 Spectro Fluorophotometer with excitation and emission bandwidths set at 5.0 nm and scan speed of 600 nm/min. A fluorescent co-gel was formed by using 10.0 mg of compound 7a (0.019 mmol, 10.0 eq.) and compound 7i (1.2 mg, 0.0019 mmol, 1.0 eq.) in 1.0 mL DMSO:H₂O (1:2). The fluorescence spectra were recorded at 350 nm as excitation wavelength. Control spectrum was recorded by preparing 1.2 mg/mL solution of 7i in DMSO:H₂O (1:2). Similar experiments were performed in acetonitrile solutions as well (Figure S3).

Naproxen trapping and release experiment: A gel was prepared in a one-dram vial using compound 7a (16.0 mg) and 0.5 mg of naproxen sodium and 2.0 mL of DMSO/H₂O (*v/v* 1:5). After a stable gel formed and the gel was left undisturbed for 15 min, 2.0 mL of water at pH 7.0 was added to the top of the gel carefully. Naproxen release from the gel was monitored by UV absorption at intervals by transferring the supernatant with a pipet to a cuvette, and after each measurement, the aqueous phase was carefully transferred back to the vial and placed on top of the gel until the next measurement. The UV spectra of the pure naproxen (0.5 mg) in 4.0 mL DMSO/H₂O (*v/v* 1:5) was also recorded as standard.

Dye absorption study: A gel was prepared in a one-dram vial using compound **7a** (16.0 mg) and 2.0 mL of DMSO/H₂O (*v/v* 1:5). After a stable gel was formed and the gel was left at room temperature for 15 min, 2.0 mL of a toluidine blue aqueous solution (0.04 mM) was added dropwise onto the top of the gel. For dye mixture absorption study, mixture of dyes prepared by using toluidine blue (0.04 mM, 1.0 mL) and methyl orange (0.024 mM, 1.0 mL) with a total volume of 2.0 mL was added on the top of the gel prepared in a similar way using compound **7a**. The adsorption of dye(s) from aqueous solution to the gel at different time intervals was monitored by UV-Vis spectroscopy.

Synthesis of sugar azide headgroup: D-glucopyranose pentaacetate **1** was synthesized following literature procedure [30,39]. This was followed by a glycosylation reaction to form compound **2** [39,40]. This compound was then treated with NaN₃ to obtain the desired azide intermediate **3** as white solid [41]. Similar procedure was followed for the synthesis of other glucose azide with three carbon spacer and galactose azides with 2 and 3 carbon spacers [42–45].

Synthesis of sugar triazole derivatives 4a–14h: These are synthesized using the CuAAC reactions either using CuSO₄·5H₂O (Method A) [31,46] or CuI (method B). Compounds **4a**, **4b**, **4e**, **7a**, **7g**, **7j**, **7k**, **11b**, **11d**, **11j** were synthesized using method A and the others were synthesized using method B. The detailed methods are shown in the ESI, only the reagents and quantities and characterization data are given.

Synthesis of compound 4a [47]: Compound **3** (70 mg, 0.17 mmol), phenyl acetylene (20.4 mg, 20 µL, 0.20 mmol), CuSO₄·5H₂O (10.0 mg, 0.04 mmol) and NaAsc (16.0 mg, 0.08 mmol). The crude product was purified with 0–2% MeOH/DCM to afford an off-white solid (86 mg, 0.165 mmol, 97%) as the desired product (*R*_f = 0.43 in 3% MeOH/DCM). m.p. 157.0–159.0 °C; ¹H NMR (400 MHz, CDCl₃) δ 7.94–7.84 (m, 3H), 7.49–7.41 (m, 2H), 7.38–7.31 (m, 1H), 5.19 (t, *J* = 9.5 Hz, 1H), 5.12–5.01 (m, 2H), 4.75–4.68 (m, 1H), 4.63–4.53 (m, 1H), 4.49 (d, *J* = 7.9 Hz, 1H), 4.34–4.25 (m, 2H), 4.16 (dd, *J* = 12.4, 2.3 Hz, 1H), 3.99–3.91 (m, 1H), 3.75–3.68 (m, 1H), 2.09 (s, 3H), 2.04 (s, 3H), 2.00 (s, 3H), 1.75 (s, 3H); ¹³C NMR (100 MHz, CDCl₃) δ 170.6, 170.0, 169.5, 169.4, (triazole at 147 ppm missing), 130.6, 128.8, 128.1, 125.7, 121.5, 100.6, 72.5, 72.0, 70.9, 68.3, 67.9, 61.7, 50.1, 20.7, 20.54, 20.51, 20.4. LC-MS (ESI+) calcd for C₂₄H₃₀N₃O₁₀ [M + H]⁺ 520 found 520.

Synthesis of compound 4b: Compound **3** (100 mg, 0.24 mmol), 1-octyne (30.8 mg, 40 µL, 0.28 mmol), CuSO₄·5H₂O (12.0 mg, 0.048 mmol) and NaAsc (22.0 mg, 0.11 mmol). The crude product was purified with 0–2% MeOH in DCM to afford an off-white solid (110.5 mg, 0.21 mmol, 87%) as the desired product (*R*_f = 0.26 in 5% MeOH/DCM). m.p. 108.0–109.0 °C; ¹H NMR (400 MHz, CDCl₃) δ 7.32 (s, 1H), 5.17 (t, *J* = 9.5 Hz, 1H), 5.07 (t, *J* = 9.8 Hz, 1H), 5.02–4.97 (m, 1H), 4.60–4.52 (m, 1H), 4.50–4.42 (m, 2H), 4.27–4.18 (m, 2H), 4.13 (dd, *J* = 12.3, 2.4 Hz, 1H), 3.95–3.87 (m, 1H), 3.73–3.65 (m, 1H), 2.76–2.61 (m, 2H), 2.08 (s, 3H), 2.02 (s, 3H), 2.00 (s, 3H), 1.95 (s, 3H), 1.71–1.61 (m, 2H), 1.41–1.26 (m, 6H), 0.88 (t, *J* = 6.9 Hz, 3H); ¹³C NMR (100 MHz, CDCl₃) δ 170.5, 170.1, 169.4, 169.2, 148.4, 122.0, 100.6, 72.5, 72.0, 71.0, 68.3, 68.0, 61.8, 49.8, 31.6, 29.4, 29.0, 25.7, 22.6, 20.7, 20.5, 14.0. LC-MS (ESI+) calcd for C₂₄H₃₈N₃O₁₀ [M + H]⁺ 528 found 528.

Synthesis of compound 4d: Compound **3** (75 mg, 0.18 mmol), 1-hexadecyne (50 mg, 62 µL, 0.22 mmol), CuI (7.0 mg, 0.036 mmol) and DIEA (35.0 mg, 47.0 µL, 0.27 mmol). The crude product was purified with 0–2% MeOH in DCM to afford an off-white solid (73.6 mg, 0.12 mmol, 67%) as the desired product (*R*_f = 0.29 in 3% MeOH/DCM). m.p. 110.0–112.0 °C; ¹H NMR (400 MHz, CDCl₃) δ 7.36 (s, 1H), 5.2 (t, *J* = 9.5 Hz, 1H), 5.09 (t, *J* = 9.8 Hz, 1H), 5.02 (dd, *J* = 9.6, 7.9 Hz, 1H), 4.62–4.56 (m, 1H), 4.54–4.45 (m, 2H), 4.31–4.20 (m, 2H), 4.16 (dd, *J* = 12.4, 2.4 Hz, 1H), 3.98–3.90 (m, 1H), 3.75–3.68 (m, 1H), 2.80–2.65 (m, 2H), 2.11 (s, 3H), 2.05 (s, 3H), 2.02 (s, 3H), 1.97 (s, 3H), 1.72–1.65 (m, 2H), 1.41–1.23 (m, 22H), 0.90 (t, *J* = 6.8 Hz, 3H); ¹³C NMR (100 MHz, CDCl₃) δ 170.5, 170.1, 169.4, 169.2, 148.5, 122.1, 100.6, 72.5, 72.0, 71.0, 68.3, 67.9, 61.8, 49.9, 31.9, 29.68, 29.65, 29.6, 29.5, 29.38, 29.37, 29.3, 25.7, 22.7, 20.7, 20.5, 14.1. LC-MS (ESI+) calcd for C₃₂H₅₄N₃O₁₀ [M + H]⁺ 640 found 640.

Synthesis of compound 4e: Compound **3** (75 mg, 0.18 mmol), 5-phenyl-1-pentyne (32 mg, 33 µL, 0.22 mmol), CuSO₄·5H₂O (9.0 mg, 0.036 mmol) and NaAsc (14.2 mg,

0.072 mmol). The crude product was purified with 0–2% MeOH in DCM to afford a white solid (98 mg, 0.17 mmol, 94%) as the desired product ($R_f = 0.37$ in 3% MeOH/DCM). m.p. 71.0–73.0 °C; $^1\text{H NMR}$ (400 MHz, CDCl_3) δ 7.37–7.29 (m, 2H), 7.28 (m, 1H), 7.23–7.16 (m, 3H), 5.19 (t, $J = 9.5$ Hz, 1H), 5.08 (t, $J = 9.9$ Hz, 1H), 5.01 (dd, $J = 9.6, 7.9$ Hz, 1H), 4.63–4.55 (m, 1H), 4.54–4.42 (m, 2H), 4.30–4.20 (m, 2H), 4.15 (dd, $J = 12.4, 2.3$ Hz, 1H), 3.97–3.89 (m, 1H), 3.74–3.68 (m, 1H), 2.81–2.67 (m, 4H), 2.09 (s, 5H), 2.04 (s, 3H), 2.02 (s, 3H), 1.92 (s, 3H); $^{13}\text{C NMR}$ (100 MHz, CDCl_3) δ 170.5, 170.1, 169.4, 169.2, 147.8, 141.8, 128.5, 128.3, 125.8, 122.1, 100.6, 72.5, 72.0, 68.3, 67.9, 61.8, 49.9, 35.4, 31.0, 25.2, 20.5. LC-MS (ESI+) calcd for $\text{C}_{27}\text{H}_{36}\text{N}_3\text{O}_{10}$ $[\text{M} + \text{H}]^+$ 562 found 562.

Synthesis of compound **4i**: Compound **3** (60 mg, 0.14 mmol), 9-ethynyl-9-fluorenone (36 mg, 0.17 mmol), CuI (11.0 mg, 0.028 mmol) and DIEA (22.3 mg, 30 μL , 0.17 mmol). The crude product was purified with 0–2% MeOH in DCM to afford a white solid (82.5 mg, 0.13 mmol, 92%) as the desired product ($R_f = 0.53$ in 5% MeOH/DCM). m.p. 101.0–104.0 °C; $^1\text{H NMR}$ (400 MHz, CDCl_3) δ 7.71–7.62 (m, 4H), 7.44–7.30 (m, 5H), 5.14 (t, $J = 9.5$ Hz, 1H), 5.03 (t, $J = 9.8$ Hz, 1H), 4.94–4.88 (m, 1H), 4.56–4.48 (m, 1H), 4.46–4.38 (m, 2H), 4.23–4.13 (m, 2H), 4.13–4.06 (m, 1H), 4.00–3.92 (m, 1H), 3.68–3.61 (m, 1H), 2.05 (s, 3H), 2.02 (s, 3H), 1.99 (s, 3H), 1.81 (s, 3H); $^{13}\text{C NMR}$ (100 MHz, CDCl_3) δ 170.6, 170.1, 169.4, 147.9, 147.8, 139.6, 129.50, 129.48, 128.4, 125.0, 124.9, 120.2, 100.4, 78.6, 72.5, 72.0, 70.9, 68.3, 67.5, 61.7, 50.1, 20.7, 20.5, 20.4. LC-MS (ESI+) calcd for $\text{C}_{31}\text{H}_{34}\text{N}_3\text{O}_{11}$ $[\text{M} + \text{H}]^+$ 624 found 624.

Synthesis of compound **7a**: Compound **6** (60 mg, 0.14 mmol), phenyl acetylene (18.6 mg, 20 μL , 0.18 mmol), $\text{CuSO}_4 \cdot 5\text{H}_2\text{O}$ (7.0 mg, 0.028 mmol) and NaAsc (11.0 mg, 0.056 mmol). The crude product was purified with 0–30% EtOAc/hexanes to afford a white solid (53.8 mg, 0.10 mmol, 71%) as the desired product ($R_f = 0.33$ in 1:3 EtOAc/hexanes). m.p. 131.0–132.0 °C; $^1\text{H NMR}$ (400 MHz, CDCl_3) δ 7.84–7.81 (m, 2H), 7.80 (s, 1H), 7.45–7.39 (m, 2H), 7.36–7.30 (m, 1H), 5.22 (t, $J = 9.5$ Hz, 1H), 5.12–5.00 (m, 2H), 4.59–4.40 (m, 3H), 4.25 (dd, $J = 12.3, 4.9$ Hz, 1H), 4.13 (dd, $J = 12.4, 2.4$ Hz, 1H), 3.92–3.83 (m, 1H), 3.73–3.66 (m, 1H), 3.59–3.49 (m, 1H), 2.31–2.14 (m, 2H), 2.08 (s, 3H), 2.032 (s, 3H), 2.027 (s, 3H), 2.01 (s, 3H); $^{13}\text{C NMR}$ (100 MHz, CDCl_3) δ 170.5, 170.2, 169.5, 169.4, 147.7, 130.6, 128.9, 128.2, 125.7, 120.2, 100.9, 72.7, 72.0, 71.3, 68.4, 65.8, 61.8, 46.6, 30.3, 20.8, 20.7, 20.6. LC-MS (ESI+) calcd for $\text{C}_{25}\text{H}_{32}\text{N}_3\text{O}_{10}$ $[\text{M} + \text{H}]^+$ 534.2 found 534.2.

Synthesis of compound **7b**: Compound **6** (70 mg, 0.16 mmol), 1-octyne (22.4 mg, 30 μL , 0.19 mmol), CuI (6.0 mg, 0.032 mmol) and DIEA (24.8 mg, 30 μL , 0.19 mmol). The crude product was purified with 0–30% EtOAc/hexanes to afford a white solid (75.6 mg, 0.14 mmol, 88%) as the desired product ($R_f = 0.23$ in 1:3 EtOAc/hexanes). m.p. 95.0–96.0 °C; $^1\text{H NMR}$ (400 MHz, CDCl_3) δ 7.26 (s, 1H), 5.21 (t, $J = 9.5$ Hz, 1H), 5.08 (t, $J = 9.7$ Hz, 1H), 5.04–4.98 (m, 1H), 4.50 (d, $J = 7.9$ Hz, 1H), 4.47–4.38 (m, 1H), 4.37–4.30 (m, 1H), 4.26 (dd, $J = 12.3, 4.8$ Hz, 1H), 4.13 (dd, $J = 12.4, 2.3$ Hz, 1H), 3.90–3.82 (m, 1H), 3.72–3.65 (m, 1H), 3.53–3.44 (m, 1H), 2.69 (t, $J = 7.7$ Hz, 2H), 2.24–2.10 (m, 2H), 2.07 (s, 6H), 2.02 (s, 3H), 2.00 (s, 3H), 1.70–1.61 (m, 2H), 1.42–1.24 (m, 6H), 0.88 (t, $J = 6.9$ Hz, 3H); $^{13}\text{C NMR}$ (100 MHz, CDCl_3) δ 170.5, 170.2, 169.4, 148.5, 120.9, 100.8, 72.8, 71.9, 71.3, 68.4, 66.0, 61.9, 46.4, 31.6, 30.3, 29.5, 29.0, 25.7, 22.6, 20.73, 20.69, 20.58, 20.57, 14.0. LC-MS (ESI+) calcd for $\text{C}_{25}\text{H}_{40}\text{N}_3\text{O}_{10}$ $[\text{M} + \text{H}]^+$ 542.3 found 542.2.

Synthesis of compound **7c**: Compound **6** (70 mg, 0.16 mmol), 1-dodecyne (32 mg, 42 μL , 0.19 mmol), CuI (6.0 mg, 0.032 mmol) and DIEA (24.8 mg, 30 μL , 0.19 mmol). The crude product was purified with 0–30% EtOAc/hexanes to afford an off white solid (62.6 mg, 0.10 mmol, 63%) as the desired product ($R_f = 0.30$ in 1:3 EtOAc/hexanes). m.p. 96.0–98.0 °C; $^1\text{H NMR}$ (400 MHz, CDCl_3) δ 7.28 (triazole 1H overlapping with CDCl_3 signal), 5.24 (t, $J = 9.5$ Hz, 1H), 5.11 (t, $J = 9.6$ Hz, 1H), 5.04 (t, $J = 9.6$ Hz, 1H), 4.53 (d, $J = 7.9$ Hz, 1H), 4.50–4.41 (m, 1H), 4.40–4.32 (m, 1H), 4.29 (dd, $J = 12.3, 4.8$ Hz, 1H), 4.16 (dd, $J = 12.4, 2.4$ Hz, 1H), 3.92–3.85 (m, 1H), 3.75–3.68 (m, 1H), 3.55–3.47 (m, 1H), 2.72 (t, $J = 7.5$ Hz, 2H), 2.27–2.12 (m, 2H), 2.10 (s, 6H), 2.05 (s, 3H), 2.04 (s, 3H), 1.74–1.64 (m, 2H), 1.41–1.23 (m, 14H), 0.90 (t, $J = 6.8$ Hz, 3H); $^{13}\text{C NMR}$ (100 MHz, CDCl_3) δ 170.5, 170.2, 169.4, 148.5, 120.9, 100.8, 72.8, 71.9, 71.3, 68.4, 66.0, 61.9, 46.4, 31.9, 30.3, 29.59, 29.56, 29.5, 29.4,

29.3, 25.7, 22.7, 20.73, 20.69, 20.6, 14.1. LC-MS (ESI+) calcd for $C_{29}H_{48}N_3O_{10}$ $[M + H]^+$ 598 found 598.

Synthesis of compound 7d: Compound **6** (70 mg, 0.16 mmol), 1-hexadecyne (40 mg, 50 μ L, 0.19 mmol), CuI (6.0 mg, 0.032 mmol) and DIEA (24.8 mg, 30 μ L, 0.19 mmol). The crude product was purified with 0–30% EtOAc/hexanes to afford a white solid (82.1 mg, 0.13 mmol, 81%) as the desired product ($R_f = 0.35$ in 1:3 EtOAc/hexanes). m.p. 101.0–103.0 $^{\circ}$ C; 1H NMR (400 MHz, $CDCl_3$) δ 7.28 (triazole 1H overlapping with $CDCl_3$ signal), 5.24 (t, $J = 9.5$ Hz, 1H), 5.11 (t, $J = 9.9$ Hz, 1H), 5.04 (dd, $J = 9.6, 8.0$ Hz, 1H), 4.53 (d, $J = 7.9$ Hz, 1H), 4.50–4.41 (m, 1H), 4.41–4.32 (m, 1H), 4.29 (dd, $J = 12.3, 4.8$ Hz, 1H), 4.16 (dd, $J = 12.4, 2.4$ Hz, 1H), 3.92–3.84 (m, 1H), 3.75–3.68 (m, 1H), 3.55–3.47 (m, 1H), 2.71 (t, $J = 7.6$ Hz, 2H), 2.21–2.12 (m, 2H), 2.10 (s, 6H), 2.05 (s, 3H), 2.03 (s, 3H), 1.73–1.61 (m, 2H), 1.42–1.21 (m, 24H), 0.90 (t, $J = 6.7$ Hz, 3H); ^{13}C NMR (100 MHz, $CDCl_3$) δ 170.5, 170.2, 169.4, 148.5, 120.9, 100.8, 72.8, 71.9, 71.3, 68.4, 66.0, 61.9, 46.4, 31.9, 30.3, 29.7, 29.6, 29.5, 29.4, 29.34, 29.33, 25.7, 22.7, 20.73, 20.69, 20.6, 14.1. LC-MS (ESI+) calcd for $C_{33}H_{56}N_3O_{10}$ $[M + H]^+$ 654 found 654.

Synthesis of compound 7e: Compound **6** (70 mg, 0.16 mmol), 5-phenyl-1-pentyne (28 mg, 30 μ L, 0.19 mmol), CuI (6.0 mg, 0.032 mmol) and DIEA (24.8 mg, 30 μ L, 0.19 mmol). The crude product was purified with 0–30% EtOAc/hexanes to afford a white solid (68.1 mg, 0.12 mmol, 75%) as the desired product ($R_f = 0.14$ in 1:3 EtOAc/hexanes). m.p. 74.0–76.0 $^{\circ}$ C; 1H NMR (400 MHz, $CDCl_3$) 7.31–7.24 (m, 3H), 7.21–7.14 (m, 3H), 5.20 (t, $J = 9.5$ Hz, 1H), 5.07 (t, $J = 9.8$ Hz, 1H), 5.04–4.98 (m, 1H), 4.49 (d, $J = 7.9$ Hz, 1H), 4.47–4.38 (m, 1H), 4.37–4.30 (m, 1H), 4.24 (dd, $J = 12.3, 4.8$ Hz, 1H), 4.12 (dd, $J = 12.3, 2.4$ Hz, 1H), 3.88–3.81 (m, 1H), 3.71–3.64 (m, 1H), 3.52–3.44 (m, 1H), 2.74 (t, $J = 7.5$ Hz, 2H), 2.69 (t, $J = 7.7$ Hz, 2H), 2.26–2.10 (m, 2H), 2.06 (s, 3H), 2.05 (s, 3H), 2.02 (s, 3H), 2.01–1.96 (m, 5H); ^{13}C NMR (100 MHz, $CDCl_3$) δ 170.5, 170.2, 169.4, 147.9, 141.9, 128.5, 128.3, 125.8, 121.1, 100.8, 72.7, 71.9, 71.3, 68.4, 66.0, 61.9, 46.4, 35.4, 31.1, 30.3, 25.2, 20.72, 20.68, 20.6. LC-MS (ESI+) calcd for $C_{28}H_{38}N_3O_{10}$ $[M + H]^+$ 576.3, found 576.2.

Synthesis of compound 7f: Compound **6** (70 mg, 0.16 mmol), propargyl alcohol (10.7 mg, 11 μ L, 0.19 mmol), CuI (6.0 mg, 0.032 mmol) and DIEA (24.8 mg, 30 μ L, 0.19 mmol). The crude product was purified with 0–30% EtOAc/hexanes to afford a light brown solid (68.8 mg, 0.14 mmol, 88%) as the desired product ($R_f = 0.1$ in 1:3 EtOAc/hexanes). m.p. 74.0–76.0 $^{\circ}$ C; 1H NMR (400 MHz, $CDCl_3$) δ 7.56 (s, 1H), 5.21 (t, $J = 9.5$ Hz, 1H), 5.09 (t, $J = 9.8$ Hz, 1H), 5.03–4.97 (m, 1H), 4.80 (s, 2H), 4.53–4.36 (m, 3H), 4.26 (dd, $J = 12.3, 4.8$ Hz, 1H), 4.17 (dd, $J = 12.3, 2.4$ Hz, 1H), 3.87–3.79 (m, 1H), 3.72–3.66 (m, 1H), 3.55–3.47 (m, 1H), 2.26–2.13 (m, 2H), 2.08 (s, 3H), 2.07 (s, 3H), 2.03 (s, 3H), 2.01 (s, 3H). ^{13}C NMR (100 MHz, $CDCl_3$) δ 170.7, 170.2, 169.5, 169.4, 147.7, 122.3, 100.7, 72.7, 72.0, 71.3, 68.4, 65.8, 61.8, 56.6, 46.7, 30.1, 20.7, 20.6. LC-MS (ESI+) calcd for $C_{20}H_{30}N_3O_{11}$ $[M + H]^+$ 488 found 488.

Synthesis of compound 7g: Compound **6** (70 mg, 0.16 mmol), 8-chloro-1-octyne (27.7 mg, 30 μ L, 0.19 mmol), $CuSO_4 \cdot 5H_2O$ (8.0 mg, 0.032 mmol) and NaAsc (13.0 mg, 0.064 mmol). The crude product was with 0–30% EtOAc/hexanes to afford a white solid (75.1 mg, 0.13 mmol, 81%) as the desired product ($R_f = 0.17$ in 1:3 EtOAc/hexanes). m.p. 74.0–76.0 $^{\circ}$ C; 1H NMR (400 MHz, $CDCl_3$) δ 7.28 (s, 1H), 5.22 (t, $J = 9.5$ Hz, 1H), 5.09 (t, $J = 9.7$ Hz, 1H), 5.05–4.99 (m, 1H), 4.51 (d, $J = 7.9$ Hz, 1H), 4.48–4.31 (m, 2H), 4.26 (dd, $J = 12.4, 4.8$ Hz, 1H), 4.14 (dd, $J = 12.3, 2.4$ Hz, 1H), 3.90–3.82 (m, 1H), 3.73–3.66 (m, 1H), 3.57–3.45 (m, 3H), 2.71 (t, $J = 7.6$ Hz, 2H), 2.25–2.10 (m, 2H), 2.08 (s, 6H), 2.03 (s, 3H), 2.01 (s, 3H), 1.83–1.74 (m, 2H), 1.73–1.65 (m, 2H), 1.52–1.44 (m, 2H), 1.43–1.36 (m, 2H); ^{13}C NMR (100 MHz, $CDCl_3$) δ 170.5, 170.2, 169.4, 148.1, 121.0, 100.8, 72.7, 71.9, 71.3, 68.4, 66.0, 61.9, 46.4, 45.0, 32.5, 30.3, 29.3, 28.4, 26.6, 25.5, 20.74, 20.70, 20.6. LC-MS (ESI+) calcd for $C_{25}H_{39}ClN_3O_{10}$ $[M + H]^+$ 576.2 found 576.2.

Synthesis of compound 7h: Compound **6** (70 mg, 0.16 mmol), 1-ethynyl-1-cyclohexanol (23 mg, 24 μ L, 0.19 mmol), CuI (6.0 mg, 0.032 mmol) and DIEA (24.8 mg, 30 μ L, 0.19 mmol). The crude product was purified with 0–30% EtOAc/hexanes to afford an off-white solid (78.9 mg, 0.14 mmol, 88%) as the desired product ($R_f = 0.10$ in 1:3 EtOAc/hexanes). m.p. 120.0–122.0 $^{\circ}$ C; 1H NMR (400 MHz, $CDCl_3$) δ 7.48 (s, 1H), 5.22 (t, $J = 9.5$ Hz, 1H), 5.11 (t,

$J = 9.9$ Hz, 1H), 5.06–5.00 (m, 1H), 4.53 (d, $J = 7.9$ Hz, 1H), 4.51–4.44 (m, 1H), 4.43–4.36 (m, 1H), 4.28 (dd, $J = 12.4, 4.7$ Hz, 1H), 4.18 (dd, $J = 12.3, 2.4$ Hz, 1H), 3.91–3.84 (m, 1H), 3.75–3.68 (m, 1H), 3.56–3.48 (m, 1H), 2.45 (s, 1H), 2.28–2.12 (m, 2H), 2.10 (s, 3H), 2.09 (s, 3H), 2.07–1.95 (m, 8H), 1.93–1.84 (m, 2H), 1.83–1.71 (m, 2H), 1.71–1.54 (m, 3H), 1.45–1.33 (m, 1H); ^{13}C NMR (100 MHz, CDCl_3) δ 170.7, 170.2, 169.5, 169.4, 146.5, 120.1, 100.8, 72.7, 72.0, 71.3, 69.6, 68.4, 66.0, 61.9, 46.6, 38.23, 38.17, 30.2, 25.4, 22.0, 20.74, 20.72, 20.6. LC-MS (ESI+) calcd for $\text{C}_{25}\text{H}_{38}\text{N}_3\text{O}_{11}$ $[\text{M} + \text{H}]^+$ 556.2 found 556.2.

Synthesis of compound **7i**: Compound **6** (100 mg, 0.24 mmol), 9-ethynyl-9-fluorenoyl (60 mg, 0.28 mmol), CuI (10.0 mg, 0.048 mmol) and DIEA (37.2 mg, 60 μL , 0.28 mmol). The crude product was purified with 0–30% EtOAc/hexanes to afford an off-white solid (121.7 mg, 0.19 mmol, 79%) as the desired product ($R_f = 0.40$ in 1:3 EtOAc/hexanes). m.p. 76.0–78.0 $^\circ\text{C}$; ^1H NMR (400 MHz, CDCl_3) δ 7.68–7.59 (m, 5H), 7.42–7.36 (m, 2H), 7.34–7.28 (m, 2H), 5.16 (t, $J = 9.5$ Hz, 1H), 5.04 (t, $J = 9.7$ Hz, 1H), 4.97–4.91 (m, 1H), 4.39–4.29 (m, 3H), 4.20 (dd, $J = 12.3, 4.8$ Hz, 1H), 4.10–4.04 (m, 1H), 3.87–3.79 (m, 1H), 3.65–3.58 (m, 1H), 3.42–3.34 (m, 1H), 2.26–2.06 (m, 2H), 2.04–2.02 (m, 6H), 2.00 (s, 3H), 1.96 (s, 3H); ^{13}C NMR (100 MHz, CDCl_3) δ 170.6, 170.1, 169.39, 169.38, 148.1, 148.0, 139.57, 139.55, 129.51, 129.48, 128.4, 124.8, 120.28, 120.26, 100.7, 78.7, 72.7, 71.9, 71.3, 68.3, 65.9, 61.8, 46.7, 30.0, 20.7, 20.61, 20.57. LC-MS (ESI+) calcd for $\text{C}_{32}\text{H}_{36}\text{N}_3\text{O}_{11}$ $[\text{M} + \text{H}]^+$ 638 found 638.

Synthesis of compound **7j**: Compound **6** (100 mg, 0.23 mmol), 8-nonynoic acid (42.5 mg, 0.28 mmol), $\text{CuSO}_4 \cdot 5\text{H}_2\text{O}$ (12.0 mg, 0.048 mmol) and NaAsc (18.2 mg, 0.092 mmol). The crude product was purified with 0–30% EtOAc/hexanes to afford a viscous liquid (112.0 mg, 0.19 mmol, 83%) as the desired product ($R_f = 0.19$ in 2% MeOH in DCM). ^1H NMR (400 MHz, $\text{DMSO}-d_6$) δ 7.80 (s, 1H), 5.33–5.20 (m, 1H), 4.91 (t, $J = 9.7$ Hz, 1H), 4.82–4.75 (m, 2H), 4.31 (t, $J = 6.8$ Hz, 2H), 4.18 (dd, $J = 12.3, 4.9$ Hz, 1H), 4.06–3.94 (m, 2H), 3.77–3.69 (m, 2H), 2.58 (t, $J = 7.5$ Hz, 2H), 2.19 (t, $J = 7.3$ Hz, 2H), 2.08–1.97 (m, 11H), 1.95 (s, 3H), 1.65–1.42 (m, 4H), 1.39–1.22 (m, 4H); ^{13}C NMR (100 MHz, $\text{DMSO}-d_6$) δ 175.0, 170.5, 170.0, 169.8, 169.6, 147.4, 122.1, 99.8, 72.5, 71.4, 71.0, 68.7, 66.4, 62.2, 46.4, 34.1, 30.2, 29.3, 28.73, 28.71, 25.4, 24.9, 20.91, 20.86, 20.81, 20.7. LC-MS (ESI+) calcd for $\text{C}_{26}\text{H}_{40}\text{N}_3\text{O}_{12}$ $[\text{M} + \text{H}]^+$ 586 found 586.

Synthesis of compound **7k**: Compound **6** (150 mg, 0.35 mmol), 1,6-heptadiyne (26 μL , 0.23 mmol), $\text{CuSO}_4 \cdot 5\text{H}_2\text{O}$ (12.0 mg, 0.046 mmol) and NaAsc (18.2 mg, 0.092 mmol). The crude product was purified with 10–80% EtOAc/hexanes to afford the monomer **7k** as a viscous liquid (46.0 mg, 0.09 mmol, 39%), together with 115.0 mg (52%) of dimeric product. ($R_f = 0.50$ in 4:1 EtOAc/hexanes). ^1H NMR (400 MHz, CDCl_3) δ 7.36 (s, 1H), 5.24 (t, $J = 9.5$ Hz, 1H), 5.11 (t, $J = 9.7$ Hz, 1H), 5.07–5.01 (m, 1H), 4.53 (d, $J = 7.9$ Hz, 1H), 4.50–4.34 (m, 2H), 4.29 (dd, $J = 12.4, 4.8$ Hz, 1H), 4.16 (dd, $J = 12.3, 2.3$ Hz, 1H), 3.91–3.83 (m, 1H), 3.75–3.68 (m, 1H), 3.54–3.46 (m, 1H), 2.86 (t, $J = 7.5$ Hz, 2H), 2.27 (dt, $J = 7.0, 2.6$ Hz, 2H), 2.24–2.12 (m, 2H), 2.10 (s, 6H), 2.05 (s, 3H), 2.03 (s, 3H), 2.00 (t, $J = 2.6$ Hz, 1H), 1.99–1.88 (m, 2H); ^{13}C NMR (100 MHz, CDCl_3) δ 170.6, 170.2, 169.4, 147.3, 121.6, 100.8, 83.8, 72.7, 72.0, 71.3, 68.9, 68.4, 66.0, 61.9, 46.5, 29.7, 28.0, 24.4, 20.74, 20.71, 20.6, 17.8. LC-MS (ESI+) calcd for $\text{C}_{24}\text{H}_{34}\text{N}_3\text{O}_{10}$ $[\text{M} + \text{H}]^+$ 524 found 524.

Synthesis of compound **11a**: Compound **10** (100 mg, 0.24 mmol), phenyl acetylene (29.4 mg, 32 μL , 0.28 mmol), CuI (10.0 mg, 0.048 mmol) and DIEA (46.5 mg, 63 μL , 0.36 mmol). The crude product was purified with 0–3% MeOH in DCM to afford a light brown viscous liquid (113 mg, 0.22 mmol, 92%) as the desired product ($R_f = 0.35$ in 5% MeOH/DCM). ^1H NMR (400 MHz, CDCl_3) δ 7.94–7.83 (m, 3H), 7.48–7.41 (m, 2H), 7.37–7.31 (m, 1H), 5.42–5.38 (m, 1H), 5.23 (dd, $J = 10.4, 7.9$ Hz, 1H), 4.99 (dd, $J = 10.5, 3.4$ Hz, 1H), 4.75–4.67 (m, 1H), 4.61–4.52 (m, 1H), 4.46 (d, $J = 7.9$ Hz, 1H), 4.36–4.27 (m, 1H), 4.22–4.09 (m, 2H), 3.98–3.87 (m, 2H), 2.16 (s, 3 H), 2.06 (s, 3 H), 1.97 (s, 3 H), 1.73 (s, 3 H); ^{13}C NMR (100 MHz, CDCl_3) δ 170.4, 170.1, 170.0, 169.7, 147.6, 130.6, 128.8, 128.1, 125.7, 121.5, 100.9, 70.9, 70.6, 68.5, 67.7, 66.9, 61.2, 50.1, 20.63, 20.59, 20.48, 20.4. LC-MS (ESI+) calcd for $\text{C}_{24}\text{H}_{30}\text{N}_3\text{O}_{10}$ $[\text{M} + \text{H}]^+$ 520.2 found 520.2.

Synthesis of compound **11b**: Compound **10** (75 mg, 0.18 mmol), 1-octyne (32 μL , 0.22 mmol), $\text{CuSO}_4 \cdot 5\text{H}_2\text{O}$ (9.0 mg, 0.04 mmol) and NaAsc (16.0 mg, 0.08 mmol). The crude

product was purified with 0–3% MeOH in DCM to afford clear viscous liquid (82 mg, 0.15 mmol, 83%) as the desired product ($R_f = 0.35$ in 5% MeOH/DCM). $^1\text{H NMR}$ (400 MHz, CDCl_3) δ 7.33 (s, 1H), 5.43–5.35 (m, 1H), 5.24–5.14 (m, 1H), 4.98 (dd, $J = 10.4, 3.3$ Hz, 1H), 4.62–4.54 (m, 1H), 4.51–4.41 (m, 2H), 4.27–4.19 (m, 1H), 4.20–4.08 (m, 2H), 3.97–3.86 (m, 2H), 2.78–2.61 (m, 2H), 2.16 (s, 3H), 2.05 (s, 3H), 1.98 (s, 3H), 1.94 (s, 3H), 1.73–1.61 (m, 2H), 1.43–1.23 (m, 6H), 0.88 (t, $J = 6.6$ Hz, 3H); $^{13}\text{C NMR}$ (100 MHz, CDCl_3) δ 170.3, 170.1, 170.0, 169.4, 148.3, 122.0, 101.0, 70.9, 70.7, 68.6, 67.9, 66.9, 61.2, 49.8, 31.6, 29.4, 29.0, 25.7, 22.6, 20.64, 20.61, 20.5, 14.0. LC-MS (ESI+) calcd for $\text{C}_{24}\text{H}_{38}\text{N}_3\text{O}_{10}$ $[\text{M} + \text{H}]^+$ 528 found 528.

Synthesis of compound **11d**: Compound **10** (75 mg, 0.18 mmol), 1-hexadecyne (48.9 mg, 0.22 mmol), $\text{CuSO}_4 \cdot 5\text{H}_2\text{O}$ (9.0 mg, 0.04 mmol) and NaAsc (16.0 mg, 0.08 mmol). The crude product was purified with 0–30% EtOAc/hexanes to afford clear viscous liquid (62 mg, 0.10 mmol, 56%) as the desired product ($R_f = 0.21$ in 1:3 EtOAc/hexanes). $^1\text{H NMR}$ (400 MHz, CDCl_3) δ 7.33 (s, 1H), 5.41–5.37 (m, 1H), 5.24–5.16 (m, 1H), 4.98 (dd, $J = 10.5, 3.4$ Hz, 1H), 4.62–4.55 (m, 1H), 4.51–4.41 (m, 2H), 4.27–4.20 (m, 1H), 4.20–4.07 (m, 2H), 3.96–3.87 (m, 2H), 2.77–2.62 (m, 2H), 2.16 (s, 3H), 2.05 (s, 3H), 1.98 (s, 3H), 1.94 (s, 3H), 1.74–1.62 (m, 2H), 1.40–1.21 (m, 22H), 0.88 (t, $J = 6.8$ Hz, 3H); $^{13}\text{C NMR}$ (100 MHz, CDCl_3) δ 170.3, 170.1, 170.0, 169.4, 148.3, 122.0, 101.0, 70.9, 70.7, 68.6, 67.9, 66.9, 61.2, 49.8, 31.9, 29.7, 29.6, 29.5, 29.4, 29.3, 25.8, 22.7, 22.6, 20.6, 20.5, 14.1. LC-MS (ESI+) calcd for $\text{C}_{32}\text{H}_{54}\text{N}_3\text{O}_{10}$ $[\text{M} + \text{H}]^+$ 640 found 640.

Synthesis of compound **11e**: Compound **10** (75 mg, 0.18 mmol), 5-phenyl-1-pentyne (32 mg, 34 μL , 0.22 mmol), CuI (7.0 mg, 0.036 mmol) and DIEA (35.0 mg, 47 μL , 0.27 mmol). The crude product was purified with 0–30% EtOAc/hexanes to afford a clear viscous liquid (95.5 mg, 0.17 mmol, 94%) as the desired product ($R_f = 0.18$ in 1:3 EtOAc/hexanes). $^1\text{H NMR}$ (400 MHz, CDCl_3) δ 7.36 (s, 1H), 7.32–7.26 (m, 2H), 7.25–7.17 (m, 3H), 5.43–5.38 (m, 1H), 5.21 (dd, $J = 10.5, 3.4$ Hz, 1H), 5.00 (dd, $J = 10.5, 3.4$ Hz, 1H), 4.65–4.55 (m, 1H), 4.53–4.44 (m, 2H), 4.29–4.22 (m, 1H), 4.21–4.10 (m, 2H), 3.98–3.88 (m, 2H), 2.83–2.67 (m, 4H), 2.15 (s, 3H), 2.06 (s, 3H), 2.05–2.01 (m, 2H), 2.00 (s, 3H), 1.92 (s, 3H); $^{13}\text{C NMR}$ (100 MHz, CDCl_3) δ 170.3, 170.1, 170.0, 169.4, 147.8, 141.9, 128.5, 128.3, 125.8, 122.1, 101.0, 70.9, 70.6, 68.6, 67.8, 66.9, 61.2, 49.8, 35.4, 31.0, 25.2, 20.63, 20.59, 20.5. LC-MS (ESI+) calcd for $\text{C}_{27}\text{H}_{36}\text{N}_3\text{O}_{10}$ $[\text{M} + \text{H}]^+$ 562 found 562.

Synthesis of compound **11i**: Compound **10** (100 mg, 0.24 mmol), 1,7-octadiyne (13 mg, 16 μL , 0.12 mmol), CuI (9.0 mg, 0.048 mmol) and DIEA (62.0 mg, 80 μL , 0.48 mmol). The crude product was purified with 0–30% EtOAc/hexanes to afford the monomer **11i** as a viscous liquid (67.7 mg, 0.13 mmol, 54%), and 31.8 mg (0.03 mmol, 28.2%) of dimer **11j** was also obtained. ($R_f = 0.26$ in 1:1 EtOAc/hexanes). $^1\text{H NMR}$ (400 MHz, CDCl_3) δ 7.37 (s, 1H), 5.43–5.38 (m, 1H), 5.24–5.17 (m, 1H), 5.03–4.97 (m, 1H), 4.64–4.55 (m, 1H), 4.53–4.43 (m, 1H), 4.29–4.21 (m, 1H), 4.20–4.10 (m, 2H), 3.97–3.89 (m, 2H), 2.81–2.65 (m, 2H), 2.47–2.15 (m, 5H), 2.06 (s, 3H), 1.99 (s, 3H), 1.97–1.94 (m, 4H), 1.78–1.68 (m, 2H), 1.64–1.46 (m, 4H). $^{13}\text{C NMR}$ (100 MHz, CDCl_3) δ 170.3, 170.1, 170.0, 169.4, 147.9, 122.1, 101.0, 84.5, 70.9, 70.6, 68.6, 68.3, 67.8, 66.9, 61.2, 49.9, 28.9, 28.4, 28.2, 25.5, 20.7, 20.63, 20.61, 20.5, 18.3. LC-MS (ESI+) calcd for $\text{C}_{25}\text{H}_{36}\text{N}_3\text{O}_{10}$ $[\text{M} + \text{Na}]^+$ 538 found 538.

Synthesis of compound **11j**: Compound **10** (100 mg, 0.24 mmol) and 1,7-octadiyne (13.6 mg, 17 μL , 0.13 mmol), $\text{CuSO}_4 \cdot 5\text{H}_2\text{O}$ (11.0 mg, 0.044 mmol) and NaAsc (17.5 mg, 0.088 mmol). The crude product was purified with 0–3% MeOH in DCM to afford a viscous liquid (86.4 mg, 0.09 mmol, 82%) as the desired product ($R_f = 0.31$ in 5% MeOH/DCM). $^1\text{H NMR}$ (400 MHz, CDCl_3) δ 7.38 (s, 2H), 5.43–5.39 (m, 2H), 5.25–5.16 (m, 2H), 5.00 (dd, $J = 10.5, 3.4$ Hz, 2H), 4.66–4.55 (m, 2H), 4.54–4.42 (m, 4H), 4.31–4.22 (m, 2H), 4.22–4.09 (m, 4H), 3.99–3.85 (m, 4H), 2.83–2.62 (m, 4H), 2.17 (s, 6H), 2.06 (s, 6H), 1.99 (s, 6H), 1.95 (s, 6H), 1.86–1.64 (m, 4H), 1.56–1.42 (m, 2H). $^{13}\text{C NMR}$ (100 MHz, CDCl_3) δ 170.3, 170.1, 170.0, 169.4, (triazole at 147 ppm missing), 122.6, 101.0, 70.9, 70.6, 68.5, 67.8, 66.9, 61.2, 49.9, 29.1, 28.9, 25.6, 20.7, 20.63, 20.61, 20.5. LC-MS (ESI+) calcd for $\text{C}_{41}\text{H}_{59}\text{N}_6\text{O}_{20}$ $[\text{M} + \text{H}]^+$ 955 found 955.

Synthesis of compound **14a**: Compound **13** (60 mg, 0.14 mmol) and phenyl acetylene (19 mg, 20 μL , 0.17 mmol), CuI (5.5 mg, 0.028 mmol) and DIEA (36.0 mg, 50 μL , 0.28 mmol). The crude product was purified with 0–30% EtOAc/hexanes to afford a semi-solid (68.8 mg,

0.13 mmol, 93%) as the desired product ($R_f = 0.37$ in 1:1 EtOAc/hexanes). ^1H NMR (400 MHz, CDCl_3) δ 7.85–7.81 (m, 2H), 7.79 (s, 1H), 7.46–7.40 (m, 2H), 7.36–7.30 (m, 1H), 5.42–5.38 (m, 1H), 5.28–5.21 (m, 1H), 5.03 (dd, $J = 10.5, 3.4$ Hz, 1H), 4.61–4.40 (m, 3H), 4.20–4.01 (m, 2H), 3.95–3.87 (m, 2H), 3.57–3.48 (m, 1H), 2.33–2.17 (m, 2H), 2.16 (s, 3H), 2.10 (s, 3H), 2.00 (s, 3H), 1.99 (s, 3H); ^{13}C NMR (100 MHz, CDCl_3) δ 170.3, 170.2, 170.1, 169.6, 147.8, 130.6, 128.9, 128.2, 125.7, 120.1, 101.4, 70.84, 70.82, 68.9, 67.0, 65.8, 61.3, 46.6, 30.3, 20.9, 20.64, 20.59, 20.55. LC-MS (ESI+) calcd for $\text{C}_{25}\text{H}_{32}\text{N}_3\text{O}_{10}$ $[\text{M} + \text{H}]^+$ 534 found 534.

Synthesis of compound 14b: Compound **13** (60 mg, 0.14 mmol), 1-octyne (18.7 mg, 25 μL , 0.17 mmol), CuI (5.5 mg, 0.028 mmol) and DIEA (36.0 mg, 50 μL , 0.28 mmol). The crude product was purified with 0–30% EtOAc/hexanes to afford a transparent viscous liquid (55.0 mg, 0.10 mmol, 71%) as the desired product ($R_f = 0.31$ in 1:1 EtOAc/hexanes). ^1H NMR (400 MHz, CDCl_3) δ 7.27 (s, 1H), 5.40–5.37 (m, 1H), 5.23–5.17 (m, 1H), 5.00 (dd, $J = 10.5, 3.4$ Hz, 1H), 4.49–4.38 (m, 2H), 4.38–4.29 (m, 1H), 4.18–4.08 (m, 2H), 3.92–3.83 (m, 2H), 3.51–3.42 (m, 1H), 2.69 (t, $J = 7.7$ Hz, 2H), 2.24–2.09 (m, 5H), 2.08 (s, 3H), 2.02 (s, 3H), 1.97 (s, 3H), 1.69–1.60 (m, 2H), 1.39–1.23 (m, 6H), 0.86 (t, $J = 7.0$ Hz, 3H); ^{13}C NMR (100 MHz, CDCl_3) δ 170.3, 170.2, 170.1, 169.6, 148.4, 120.9, 101.3, 70.8, 70.8, 68.9, 67.0, 65.9, 61.2, 46.5, 31.5, 30.3, 29.4, 28.9, 25.6, 22.5, 20.8, 20.6, 20.5, 14.0. LC-MS (ESI+) calcd for $\text{C}_{25}\text{H}_{40}\text{N}_3\text{O}_{10}$ $[\text{M} + \text{H}]^+$ 542.2 found 542.2.

Synthesis of compound 14c: Compound **13** (60 mg, 0.14 mmol), 1-dodecyne (29 mg, 38 μL , 0.17 mmol) CuI (5.5 mg, 0.028 mmol) and DIEA (36.0 mg, 50 μL , 0.28 mmol). The crude product was purified with 0–30% EtOAc/hexanes to afford a white solid (48.9 mg, 0.08 mmol, 57%) as the desired product ($R_f = 0.28$ in 1:1 EtOAc/hexanes). m.p. 65.0–66.0 $^\circ\text{C}$; ^1H NMR (400 MHz, CDCl_3) δ 7.26 (triazole 1H under CDCl_3 signal), 5.43–5.38 (m, 1H), 5.26–5.19 (m, 1H), 5.03 (dd, $J = 10.4, 3.5$ Hz, 1H), 4.49–4.40 (m, 2H), 4.38–4.30 (m, 1H), 4.19–4.11 (m, 2H), 3.94–3.86 (m, 2H), 3.52–3.44 (m, 1H), 2.70 (t, $J = 7.7$ Hz, 2H), 2.24–2.11 (m, 5H), 2.10 (s, 3H), 2.04 (s, 3H), 1.99 (s, 3H), 1.71–1.62 (m, 2H), 1.41–1.21 (m, 14H), 0.88 (t, $J = 6.6$ Hz, 3H); ^{13}C NMR (100 MHz, CDCl_3) δ 170.3, 170.2, 170.1, 169.6, 148.5, 120.8, 101.3, 70.84, 70.78, 68.9, 67.0, 66.0, 61.2, 46.4, 31.9, 30.3, 29.59, 29.56, 29.5, 29.4, 29.3, 25.7, 22.7, 20.9, 20.63, 20.55, 14.1. LC-MS (ESI+) calcd for $\text{C}_{29}\text{H}_{48}\text{N}_3\text{O}_{10}$ $[\text{M} + \text{H}]^+$ 598.3 found 598.4.

Synthesis of compound 14d: Compound **13** (60 mg, 0.14 mmol), 1-hexadecyne (38.5 mg, 48 μL , 0.17 mmol), CuI (5.5 mg, 0.028 mmol) and DIEA (36.0 mg, 50 μL , 0.28 mmol). The crude product was purified with 0–30% EtOAc/hexanes to afford a white solid (68.8 mg, 0.11 mmol, 79%) as the desired product ($R_f = 0.43$ in 3% MeOH/DCM). m.p. 77.0–78.0 $^\circ\text{C}$; ^1H NMR (400 MHz, CDCl_3) δ 7.25 (s, 1H), 5.43–5.37 (m, 1H), 5.25–5.18 (m, 1H), 5.02 (dd, $J = 10.5, 3.4$ Hz, 1H), 4.51–4.39 (m, 1H), 4.38–4.29 (m, 1H), 4.19–4.09 (m, 2H), 3.96–3.84 (m, 2H), 3.52–3.43 (m, 1H), 2.69 (t, $J = 7.6$ Hz, 2H), 2.22–2.12 (m, 5H), 2.09 (s, 3H), 2.03 (s, 3H), 1.99 (s, 3H), 1.73–1.60 (m, 2H), 1.40–1.20 (m, 22H), 0.88 (t, $J = 6.9$ Hz, 3H); ^{13}C NMR (100 MHz, CDCl_3) δ 170.3, 170.2, 170.1, 169.6, 148.5, 120.8, 101.3, 70.84, 70.78, 68.9, 67.0, 66.0, 61.2, 46.4, 31.9, 30.3, 29.7, 29.6, 29.5, 29.4, 29.3, 25.7, 22.7, 20.9, 20.6, 20.5, 14.1. LC-MS (ESI+) calcd for $\text{C}_{33}\text{H}_{56}\text{N}_3\text{O}_{10}$ $[\text{M} + \text{H}]^+$ 654.4 found 654.4.

Synthesis of compound 14e: Compound **13** (60 mg, 0.14 mmol), 5-phenyl-1-pentyne (24.5 mg, 25 μL , 0.17 mmol) CuI (5.5 mg, 0.028 mmol) and DIEA (21.7 mg, 30 μL , 0.17 mmol). The crude product was purified with 0–50% EtOAc/hexanes to afford a transparent viscous liquid (56.2 mg, 0.10 mmol, 71%) as the desired product ($R_f = 0.29$ in 1:1 EtOAc/hexanes). ^1H NMR (400 MHz, CDCl_3) δ 7.31–7.26 (m, 3H), 7.21–7.15 (m, 3H), 5.42–5.37 (m, 1H), 5.25–5.18 (m, 1H), 5.02 (dd, $J = 10.5, 3.4$ Hz, 1H), 4.50–4.40 (m, 2H), 4.39–4.30 (m, 1H), 4.18–4.08 (m, 2H), 3.92–3.85 (m, 2H), 3.52–3.43 (m, 1H), 2.75 (t, $J = 7.7$ Hz, 2H), 2.70 (t, $J = 7.6$ Hz, 2H), 2.24–2.11 (m, 5H), 2.08 (s, 3H), 2.06–2.01 (m, 5H), 1.99 (s, 3H); ^{13}C NMR (100 MHz, CDCl_3) δ 170.3, 170.2, 170.1, 169.6, 147.9, 141.9, 128.5, 128.3, 125.9, 121.0, 101.3, 70.83, 70.79, 68.9, 67.0, 65.9, 61.2, 46.5, 35.4, 31.1, 30.3, 25.2, 20.9, 20.63, 20.55. LC-MS (ESI+) calcd for $\text{C}_{28}\text{H}_{38}\text{N}_3\text{O}_{10}$ $[\text{M} + \text{H}]^+$ 576.2 found 576.2.

Synthesis of compound 14f: Compound **13** (60 mg, 0.14 mmol), 8-chloro-1-octyne (24.6 mg, 28 μL , 0.17 mmol), $\text{CuSO}_4 \cdot 5\text{H}_2\text{O}$ (7.0 mg, 0.028 mmol), NaAsc (11.0 mg, 0.056 mmol). The crude product was purified with 0–50% EtOAc/hexanes to afford a semi solid (56.2 mg,

0.10 mmol, 71%) as the desired product. $R_f = 0.14$ in 1:1 EtOAc/hexanes; $^1\text{H NMR}$ (400 MHz, CDCl_3) δ 7.27 (s, 1H), 5.42–5.36 (m, 1H), 5.25–5.18 (m, 1H), 5.02 (dd, $J = 10.5, 3.4$ Hz, 1H), 4.50–4.39 (m, 2H), 4.38–4.30 (m, 1H), 4.19–4.08 (m, 2H), 3.94–3.83 (m, 2H), 3.52 (t, $J = 6.7$ Hz, 2H), 3.50–3.46 (m, 1H), 2.70 (t, $J = 7.6$ Hz, 2H), 2.23–2.10 (m, 5H), 2.09 (s, 3H), 2.03 (s, 3H), 1.98 (s, 3H), 1.81–1.73 (m, 2H), 1.73–1.62 (m, 2H), 1.52–1.43 (m, 2H), 1.43–1.34 (m, 2H); $^{13}\text{C NMR}$ (100 MHz, CDCl_3) δ 169.3, 169.2, 169.1, 168.6, 147.1, 119.9, 100.3, 69.83, 69.78, 67.9, 66.0, 65.0, 60.2, 45.4, 44.0, 31.5, 29.3, 28.3, 27.4, 25.6, 24.5, 19.9, 19.6, 19.5. LC-MS (ESI+) calcd for $\text{C}_{25}\text{H}_{39}\text{ClN}_3\text{O}_{10}$ $[\text{M} + \text{H}]^+$ 577 found 577.

Synthesis of compound 14g: Compound **13** (60 mg, 0.14 mmol), propargyl alcohol (9.5 mg, 0.17 mmol), CuI (5.5 mg, 0.028 mmol), DIEA (21.7 mg, 0.17 mmol). The crude was purified with 0–5% MeOH in DCM to afford a viscous liquid (55.8 mg, 0.11 mmol, 79%) as the desired product ($R_f = 0.25$ in 5% MeOH/DCM). $^1\text{H NMR}$ (400 MHz, CDCl_3) δ 7.56 (s, 1H), 5.39–5.35 (m, 1H), 5.20–5.14 (m, 1H), 5.00 (dd, $J = 10.5, 3.4$ Hz, 1H), 4.76 (s, 2H), 4.50–4.34 (m, 3H), 4.20–4.13 (m, 1H), 4.12–4.05 (m, 1H), 3.92–3.81 (m, 2H), 3.52–3.44 (m, 1H), 2.26–2.10 (m, 5H), 2.06 (s, 3H), 2.01 (s, 3H), 1.96 (s, 3H); $^{13}\text{C NMR}$ (100 MHz, CDCl_3) δ 170.5, 170.2, 170.1, 169.7, 147.7, 122.3, 101.1, 70.8, 68.9, 67.1, 65.8, 61.3, 56.4, 46.8, 30.1, 20.8, 20.6, 20.5. LC-MS (ESI+) calcd for $\text{C}_{20}\text{H}_{30}\text{N}_3\text{O}_{11}$ $[\text{M} + \text{H}]^+$ 488.2 found 488.2.

Synthesis of compound 14h: Compound **13** (70 mg, 0.16 mmol), 1-ethynyl-1-cyclohexanol (23.8 mg, 0.19 mmol), CuI (6.1 mg, 0.032 mmol) and DIEA (24.8 mg, 0.19 mmol). The crude was purified with 0–50% EtOAc/hexanes to afford a semi-solid (61.3 mg, 0.11 mmol, 69%) as the desired product ($R_f = 0.17$ in 1:1 EtOAc/hexanes). $^1\text{H NMR}$ (400 MHz, CDCl_3) δ 7.48 (s, 1H), 5.42–7.36 (m, 1H), 5.24–5.16 (m, 1H), 5.02 (dd, $J = 10.5, 3.4$ Hz, 1H), 4.51–4.33 (m, 3H), 4.21–4.06 (m, 2H), 3.94–3.83 (m, 2H), 3.54–3.45 (m, 1H), 2.57 (br s, 1H), 2.23–2.09 (m, 5H), 2.08 (s, 3H), 2.03 (s, 3H), 1.98–1.93 (m, 4H), 1.91–1.82 (m, 2H), 1.81–1.68 (m, 2H), 1.67–1.47 (m, 4H), 1.42–1.30 (m, 1H); $^{13}\text{C NMR}$ (100 MHz, CDCl_3) δ 170.4, 170.2, 170.0, 169.6, 120.1, 101.2, 70.8, 69.5, 68.9, 67.0, 65.9, 61.3, 46.6, 38.2, 30.2, 25.4, 22.0, 20.83, 20.77, 20.69, 20.6, 20.5. LC-MS (ESI+) calcd for $\text{C}_{25}\text{H}_{38}\text{N}_3\text{O}_{11}$ $[\text{M} + \text{H}]^+$ 556.2 found 556.2.

4. Conclusions

We have synthesized and characterized four series of peracetylated β -triazolyl alkyl glycosides of D-glucose and D-galactose with two and three carbon spacers. Several effective gelators were obtained from the glucose derivatives and the gels were characterized using optical microscopy, AFM, UV-Vis, FTIR spectroscopies and rheology. The glycoside triazole derivatives with two and three carbon spacers having aromatic ring or the long hydrophobic chains attached to the triazole ring were found to be effective gelators in aqueous mixtures of DMSO and ethanol. The gelator **7a** was able to form gels in 17% DMSO aqueous solution and the gel was able to encapsulate a drug (naproxen sodium) and form a co-gel which was further analyzed for its sustained release from the gel to the aqueous phase. The compound **7a** also formed metallo gels with several different metal ions, the gels were analyzed by FTIR spectroscopy. Moreover, the co-gel of the Fmoc derivative **7i** with the gelator **7a** exhibited enhanced fluorescence upon gelation, which could be utilized as a probe for understanding the gelation mechanism and other studies. The powder XRD patterns of the xerogels indicated certain crystallinity in the gel phase. The use of galactose seems to diminish the gelation tendencies of triazolyl glycosides. This suggests that for designing effective gelators, the polarity of the triazole group should be balanced by introducing hydrophobic chains or aromatic groups which is evident from this study. We believe that these novel molecules obtained by systematically studying the effects of various structural features for this series will help in the development of effective LMWGs for various applications.

Supplementary Materials: The following are available online at <https://www.mdpi.com/article/10.3390/chemistry3030068/s1>, Copies of ¹H and ¹³C NMR spectra and some 2D NMR spectra (Part I), detailed gel test tables (Tables S1 and S2), additional AFM images (Figure S2), UV, fluorescence (Figure S3), procedures for water dilution (Tables S3 and S4), naproxen release study (Figure S4), dye absorption study (Figures S5–S8), rheology data (Tables S6–S10), IR spectra of various compounds (Figure S9), PXRD data (Figures S10 and S11, Tables S11 and S12) and pH stability studies (Figures S13 and S14).

Author Contributions: Conceptualization, G.W.; methodology, G.W., P.S.; validation, G.W.; A.C. and P.S.; formal analysis, G.W., P.S.; investigation, P.S.; resources, G.W.; data curation, P.S. and D.W.; writing—original draft preparation, P.S., G.W.; writing—review and editing, G.W., P.S. and A.C.; supervision, G.W., funding acquisition, G.W. All authors have read and agreed to the published version of the manuscript.

Funding: We thank the financial support from National Science Foundation grants CHE 1808609.

Institutional Review Board Statement: Not applicable.

Informed Consent Statement: Not applicable.

Data Availability Statement: Not applicable.

Acknowledgments: We thank Silvina Pagola for her assistance with XRD experiments and Venkat Maruthamuthu and Mazen Mezher for assistance with Rheological experiments.

Conflicts of Interest: The authors declare no conflict of interest.

References

1. Du, X.; Zhou, J.; Shi, J.; Xu, B. Supramolecular hydrogelators and hydrogels: From soft matter to molecular biomaterials. *Chem. Rev.* **2015**, *115*, 13165–13307. [[CrossRef](#)]
2. Babu, S.S.; Praveen, V.K.; Ajayaghosh, A. Functional π -gelators and their applications. *Chem. Rev.* **2014**, *114*, 1973–2129. [[CrossRef](#)]
3. Terech, P.; Weiss, R.G. Low molecular mass gelators of organic liquids and the properties of their gels. *Chem. Rev.* **1997**, *97*, 3133–3160. [[CrossRef](#)] [[PubMed](#)]
4. Estroff, L.A.; Hamilton, A.D. Water gelation by small organic molecules. *Chem. Rev.* **2004**, *104*, 1201–1217. [[CrossRef](#)] [[PubMed](#)]
5. Diaz Diaz, D.; Kuhbeck, D.; Koopmans, R.J. Stimuli-responsive gels as reaction vessels and reusable catalysts. *Chem. Soc. Rev.* **2011**, *40*, 427–448. [[CrossRef](#)]
6. Shigemitsu, H.; Hamachi, I. Design Strategies of stimuli-responsive supramolecular hydrogels relying on structural analyses and cell-mimicking approaches. *Acc. Chem. Res.* **2017**, *50*, 740–750. [[CrossRef](#)]
7. Zhang, J.; Su, C.-Y. Metal-organic gels: From discrete metallogelators to coordination polymers. *Coord. Chem. Rev.* **2013**, *257*, 1373–1408. [[CrossRef](#)]
8. He, L.; Peng, Z.W.; Jiang, Z.W.; Tang, X.Q.; Huang, C.Z.; Li, Y.F. Novel iron(III)-based metal-organic gels with superior catalytic performance toward luminol chemiluminescence. *ACS Appl. Mater. Interfaces* **2017**, *9*, 31834–31840. [[CrossRef](#)]
9. Wu, H.; Zheng, J.; Kjoniksen, A.L.; Wang, W.; Zhang, Y.; Ma, J. Metallogels: Availability, applicability, and advanceability. *Adv. Mater.* **2019**, *31*, e1806204. [[CrossRef](#)] [[PubMed](#)]
10. Liu, J.; Fan, Y.-Q.; Song, S.-S.; Gong, G.-F.; Wang, J.; Guan, X.-W.; Yao, H.; Zhang, Y.-M.; Wei, T.-B.; Lin, Q. Aggregation-Induced Emission Supramolecular Organic Framework (AIE SOF) gels constructed from supramolecular polymer networks based on tripodal pillar[5]arene for fluorescence detection and efficient removal of various analytes. *ACS Sustain. Chem. Eng.* **2019**, *7*, 11999–12007. [[CrossRef](#)]
11. Yang, Z.; Xu, B. A simple visual assay based on small molecule hydrogels for detecting inhibitors of enzymes. *Chem. Commun.* **2004**, *10*, 2424–2425. [[CrossRef](#)] [[PubMed](#)]
12. Yang, Z.; Xu, B. Using enzymes to control molecular hydrogelation. *Adv. Mater.* **2006**, *18*, 3043–3046. [[CrossRef](#)]
13. Toledano, S.; Williams, R.J.; Jayawarna, V.; Ulijn, R.V. Enzyme-Triggered self-assembly of peptide hydrogels via reversed hydrolysis. *J. Am. Chem. Soc.* **2006**, *128*, 1070–1071. [[CrossRef](#)]
14. Pires, R.A.; Abul-Haija, Y.M.; Costa, D.S.; Novoa-Carballal, R.; Reis, R.L.; Ulijn, R.V.; Pashkuleva, I. Controlling cancer cell fate using localized biocatalytic self-assembly of an aromatic carbohydrate amphiphile. *J. Am. Chem. Soc.* **2015**, *137*, 576–579. [[CrossRef](#)] [[PubMed](#)]
15. Xie, Y.-Y.; Qin, X.-T.; Feng, J.-Y.; Zhong, C.; Jia, S.-R. A self-assembled amino acid-based hydrogel with broad-spectrum antibacterial activity. *J. Mater. Sci.* **2021**, *56*, 7626–7636. [[CrossRef](#)]
16. Yang, Z.-y.; Zhong, Y.-y.; Zheng, J.; Liu, Y.; Li, T.; Hu, E.; Zhu, X.-f.; Ding, R.-q.; Wu, Y.; Zhang, Y. Fmoc-amino acid-based hydrogel vehicle for delivery of amygdalin to perform neuroprotection. *Smart Mater. Med.* **2021**, *2*, 56–64. [[CrossRef](#)]
17. Kadeeja, A.; Joseph, S.; Abraham, J.N. Self-assembly of novel Fmoc-cardanol compounds into hydrogels—Analysis based on rheological, structural and thermal properties. *Soft Matter* **2020**, *16*, 6294–6303. [[CrossRef](#)]

18. Datta, S.; Bhattacharya, S. Multifarious facets of sugar-derived molecular gels: Molecular features, mechanisms of self-assembly and emerging applications. *Chem. Soc. Rev.* **2015**, *44*, 5596–5637. [[CrossRef](#)]
19. Prathap, A.; Sureshan, K.M. Sugar-Based organogelators for various applications. *Langmuir* **2019**, *35*, 6005–6014. [[CrossRef](#)] [[PubMed](#)]
20. Morris, J.; Bietsch, J.; Bashaw, K.; Wang, G. Recently developed carbohydrate based gelators and their applications. *Gels* **2021**, *7*, 24. [[CrossRef](#)]
21. Fan, K.; Wang, X.; Wang, X.; Yang, H.; Han, G.; Zhou, L.; Fang, S. One-step-synthesized D-gluconic acetal-based supramolecular organogelators with effective phase-selective gelation. *RSC Adv.* **2020**, *10*, 37080–37085. [[CrossRef](#)]
22. Zhang, B.; Chen, S.; Luo, H.; Zhang, B.; Wang, F.; Song, J. Porous amorphous powder form phase-selective organogelator for rapid recovery of leaked aromatics and spilled oils. *J. Hazard. Mater.* **2020**, *384*, 121460. [[CrossRef](#)]
23. Tiwari, V.K.; Mishra, B.B.; Mishra, K.B.; Mishra, N.; Singh, A.S.; Chen, X. Cu-Catalyzed click reaction in carbohydrate chemistry. *Chem. Rev.* **2016**, *116*, 3086–3240. [[CrossRef](#)] [[PubMed](#)]
24. He, X.-P.; Zeng, Y.-L.; Zang, Y.; Li, J.; Field, R.A.; Chen, G.-R. Carbohydrate CuAAC click chemistry for therapy and diagnosis. *Carbohydr. Res.* **2016**, *429*, 1–22. [[CrossRef](#)] [[PubMed](#)]
25. Thirumurugan, P.; Matosiuk, D.; Jozwiak, K. Click chemistry for drug development and diverse chemical-biology applications. *Chem. Rev.* **2013**, *113*, 4905–4979. [[CrossRef](#)] [[PubMed](#)]
26. Schulze, B.; Schubert, U.S. Beyond click chemistry—Supramolecular interactions of 1,2,3-triazoles. *Chem. Soc. Rev.* **2014**, *43*, 2522–2571. [[CrossRef](#)]
27. Bozorov, K.; Zhao, J.; Aisa, H.A. 1,2,3-Triazole-containing hybrids as leads in medicinal chemistry: A recent overview. *Bioorg. Med. Chem.* **2019**, *27*, 3511–3531. [[CrossRef](#)] [[PubMed](#)]
28. Okafor, I.S.; Wang, G. Synthesis and gelation property of a series of disaccharide triazole derivatives. *Carbohydr. Res.* **2017**, *451*, 81–94. [[CrossRef](#)] [[PubMed](#)]
29. Chen, A.; Okafor, I.S.; Garcia, C.; Wang, G. Synthesis and self-assembling properties of 4,6-O-benzylidene acetal protected D-glucose and D-glucosamine β -1,2,3-triazole derivatives. *Carbohydr. Res.* **2018**, *461*, 60–75. [[CrossRef](#)] [[PubMed](#)]
30. Mangunuru, H.P.R.; Yerabolu, J.R.; Liu, D.; Wang, G. Synthesis of a series of glucosyl triazole derivatives and their self-assembling properties. *Tetrahedron Lett.* **2015**, *56*, 82–85. [[CrossRef](#)]
31. Mangunuru, H.P.R.; Yerabolu, J.R.; Wang, G. Synthesis and study of N-acetyl D-glucosamine triazole derivatives as effective low molecular weight gelators. *Tetrahedron Lett.* **2015**, *56*, 3361–3364. [[CrossRef](#)]
32. Chen, A.; Wang, D.; Bietsch, J.; Wang, G. Synthesis and characterization of pentaerythritol derived glycoconjugates as supramolecular gelators. *Org. Biomol. Chem.* **2019**, *17*, 6043–6056. [[CrossRef](#)] [[PubMed](#)]
33. Wang, G.; Wang, D.; Bietsch, J.; Chen, A.; Sharma, P. Synthesis of dendritic glycoclusters and their applications for supramolecular gelation and catalysis. *J. Org. Chem.* **2020**, *85*, 16136–16156. [[CrossRef](#)]
34. Narayana, C.; Kumari, P.; Tiwari, G.; Sagar, R. Triazole linked N-Acetylglucosamine based gelators for crude oil separation and dye removal. *Langmuir* **2019**, *35*, 16803–16812. [[CrossRef](#)] [[PubMed](#)]
35. Pathak, N.P.; Chatterjee, D.; Paul, A.; Yadav, S. Arabinose based gelators: Rheological characterization of the gels and phase selective organogelation of crude-oil. *RSC Adv.* **2016**, *6*, 92225–92234. [[CrossRef](#)]
36. Kazarian, S.G.; Chan, K.L.A. Micro- and macro-attenuated total reflection Fourier transform infrared spectroscopic imaging. *Appl. Spectrosc.* **2010**, *64*, 135A–152A. [[CrossRef](#)]
37. Chen, Y.; Lam, J.W.; Kwok, R.T.; Liu, B.; Tang, B.Z. Aggregation-induced emission: Fundamental understanding and future developments. *Mater. Horiz.* **2019**, *6*, 428–433. [[CrossRef](#)]
38. Chen, Y.-Y.; Gong, G.-F.; Fan, Y.-Q.; Zhou, Q.; Zhang, Q.-P.; Yao, H.; Zhang, Y.-M.; Wei, T.-B.; Lin, Q. A novel AIE-based supramolecular polymer gel serves as an ultrasensitive detection and efficient separation material for multiple heavy metal ions. *Soft Matter* **2019**, *15*, 6878–6884. [[CrossRef](#)]
39. Husain, A.A.; Maknenko, A.M.; Bisht, K.S. Spatially directional resorcin[4]arene cavitand glycoconjugates for organic catalysis. *Chem.-Eur. J.* **2016**, *22*, 6223–6227. [[CrossRef](#)]
40. Ma, J.; Yang, X.; Hao, W.; Huang, Z.; Wang, X.; Wang, P.G. Mono-functionalized glycosylated platinum(IV) complexes possessed both pH and redox dual-responsive properties: Exhibited enhanced safety and preferentially accumulated in cancer cells in vitro and in vivo. *Eur. J. Med. Chem.* **2017**, *128*, 45–55. [[CrossRef](#)]
41. Husain, A.A.; Bisht, K.S. Synthesis of a novel resorcin[4]arene-glucose conjugate and its catalysis of the CuAAC reaction for the synthesis of 1,4-disubstituted 1,2,3-triazoles in water. *RSC Adv.* **2019**, *9*, 10109–10116. [[CrossRef](#)]
42. Zhang, P.; Ma, J.; Zhang, Q.; Jian, S.; Sun, X.; Liu, B.; Nie, L.; Liu, M.; Liang, S.; Zeng, Y.; et al. Monosaccharide analogues of anticancer peptide r-lycosin-i: Role of monosaccharide conjugation in complexation and the potential of lung cancer targeting and therapy. *J. Med. Chem.* **2019**, *62*, 7857–7873. [[CrossRef](#)] [[PubMed](#)]
43. Cervin, J.; Boucher, A.; Youn, G.; Bjoerklund, P.; Wallenius, V.; Mottram, L.; Sampson, N.S.; Yrlid, U. Fucose-Galactose polymers inhibit cholera toxin binding to fucosylated structures and galactose-dependent intoxication of human enteroids. *ACS Infect. Dis.* **2020**, *6*, 1192–1203. [[CrossRef](#)]
44. Wang, Y.-Y.; El-Boubbou, K.; Kouyoumdjian, H.; Sun, B.; Huang, X.-F.; Zeng, X.-Q. Lipoic acid glyco-conjugates, a new class of agents for controlling nonspecific adsorption of blood serum at biointerfaces for Biosensor and Biomedical Applications. *Langmuir* **2010**, *26*, 4119–4125. [[CrossRef](#)] [[PubMed](#)]

-
45. Joosten, J.A.F.; Loimaranta, V.; Appeldoorn, C.C.M.; Haataja, S.; El Maate, F.A.; Liskamp, R.M.J.; Finne, J.; Pieters, R.J. Inhibition of streptococcus suis adhesion by dendritic galabiose compounds at low nanomolar concentration. *J. Med. Chem.* **2004**, *47*, 6499–6508. [[CrossRef](#)]
 46. Wang, G.; Chen, A.; Mangunuru, H.P.R.; Yerabolu, J.R. Synthesis and characterization of amide linked triazolyl glycolipids as molecular hydrogelators and organogelators. *RSC Adv.* **2017**, *7*, 40887–40895. [[CrossRef](#)]
 47. Thorwirth, R.; Stolle, A.; Ondruschka, B.; Wild, A.; Schubert, U.S. Fast, ligand- and solvent-free copper-catalyzed click reactions in a ball mill. *Chem. Commun.* **2011**, *47*, 4370–4372. [[CrossRef](#)]